

Implementation of the frozen-spin technique for the search for a muon EDM

– *New Frontiers in Lepton Flavor (Pisa, May 2023)* –

Tim Hume

Supervisor: Dr. Philipp Schmidt-Wellenburg

ETH zürich

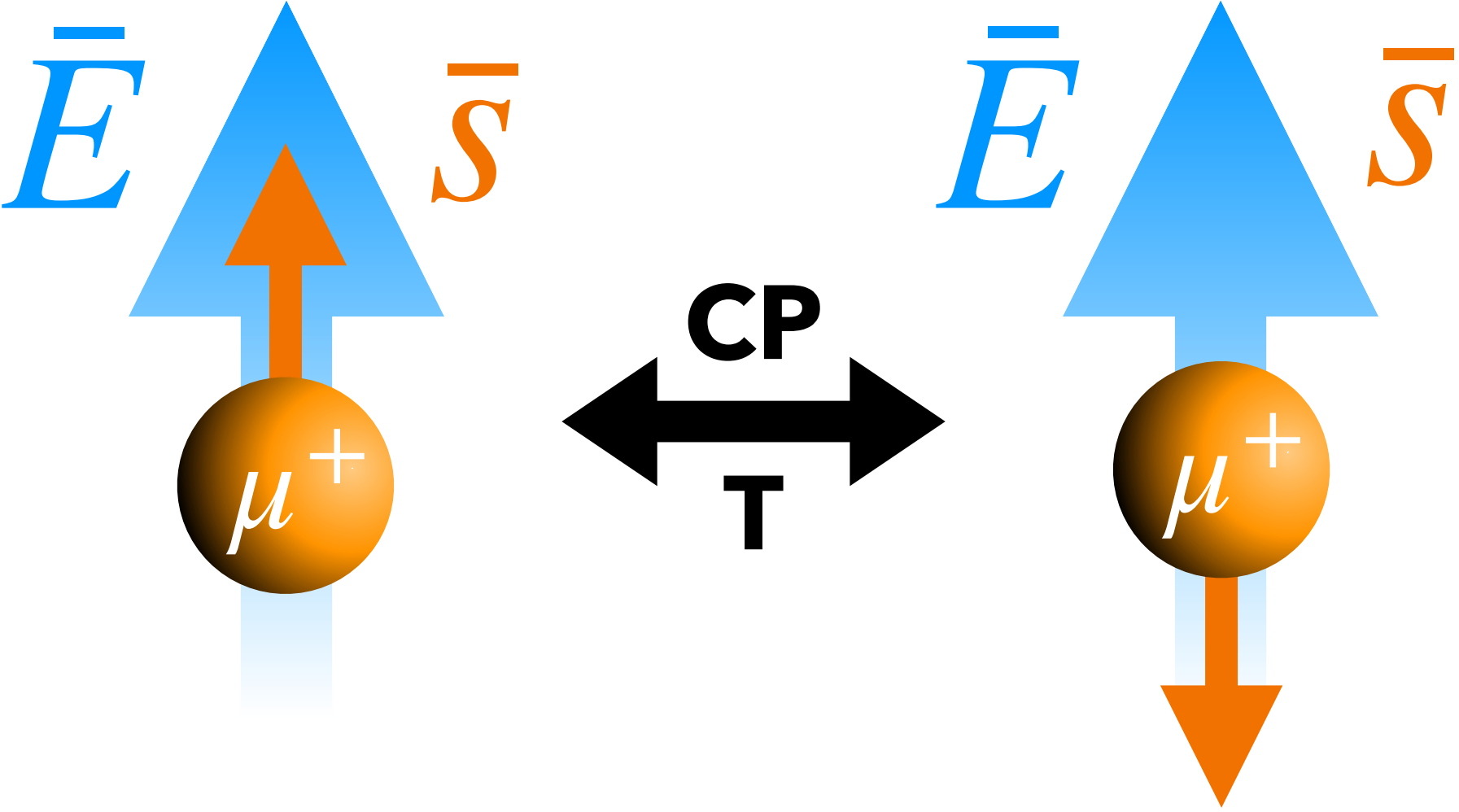
PAUL SCHERRER INSTITUT
PSI



timothy.hume@psi.ch

muEDM Experiment @ PSI

A permanent EDM requires T violation,
equivalently CP violation by the CPT Theorem.

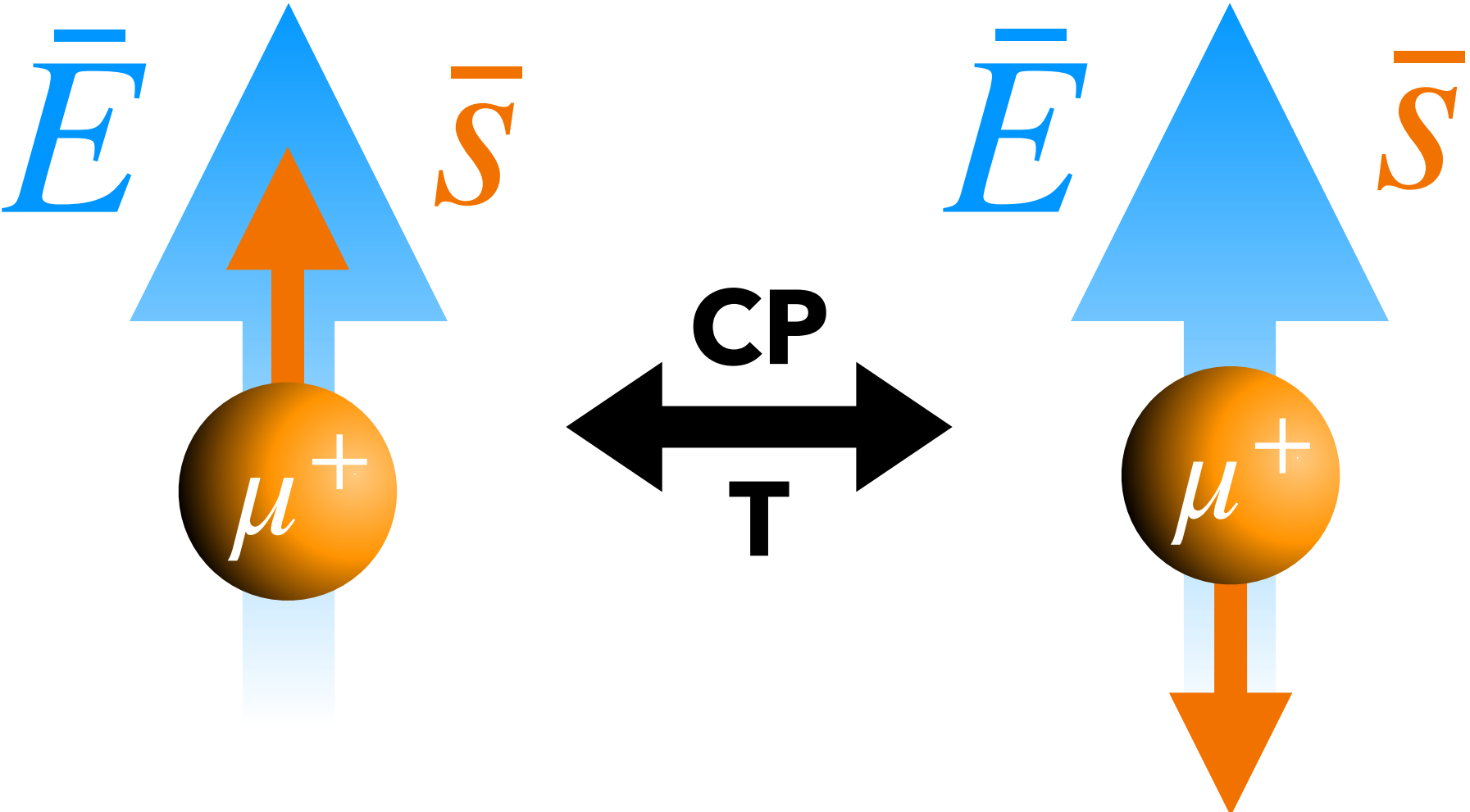


$$H_{\mu}^{EDM} \stackrel{\beta \rightarrow 0}{\propto} d_{\mu} \bar{\sigma} \cdot \bar{E}$$

Hamiltonian EDM term is CP violating

muEDM Experiment @ PSI

A permanent EDM requires T violation,
equivalently CP violation by the CPT Theorem.



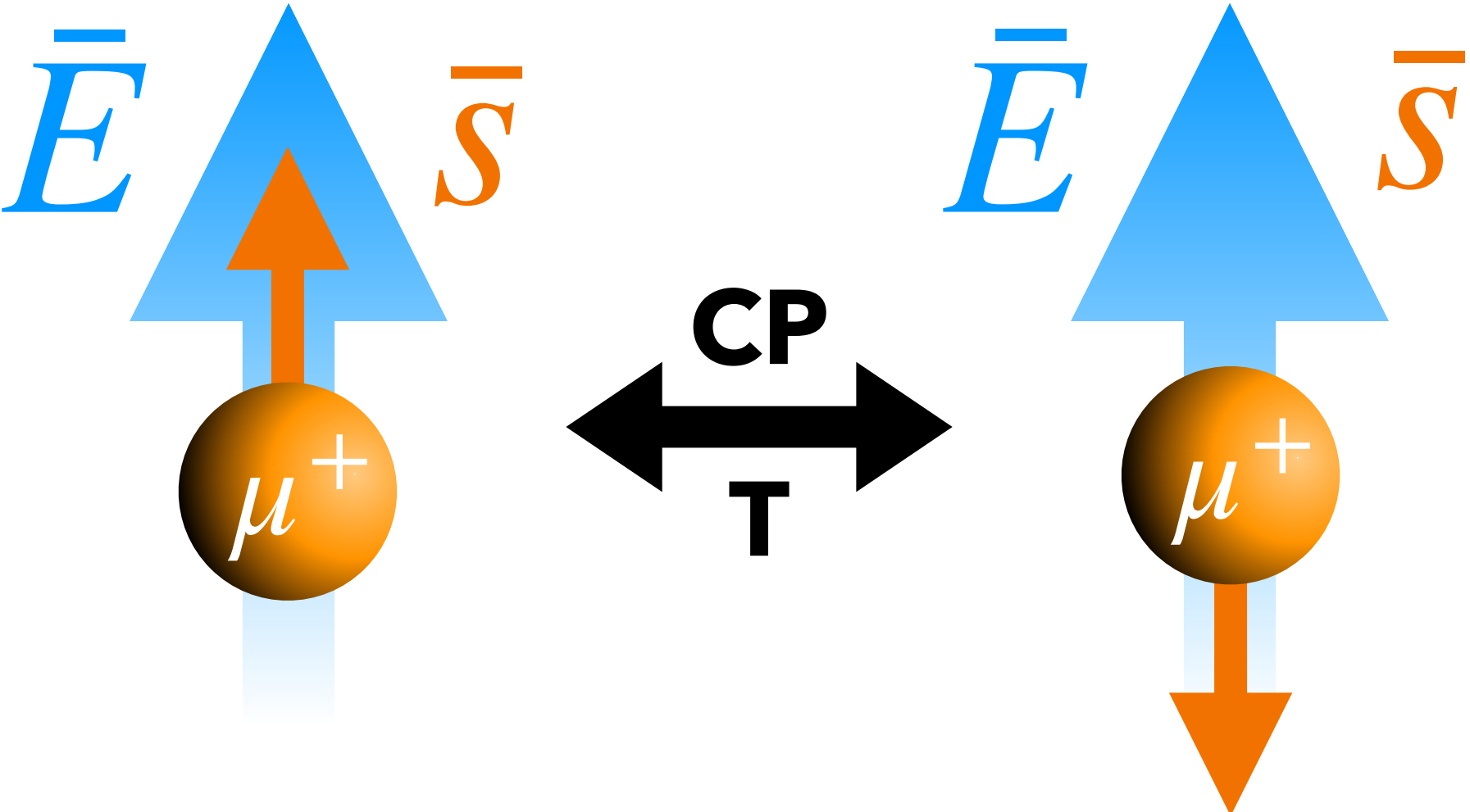
$$H_{\mu}^{EDM} \stackrel{\beta \rightarrow 0}{\propto} d_{\mu} \bar{\sigma} \cdot \bar{E}$$

Hamiltonian EDM term is CP violating

SM Prediction: $d_{\mu}^{SM} = 1.4 \times 10^{-38} e \cdot cm$ (Yamaguchi & Yamanaka, 2020)

muEDM Experiment @ PSI

A permanent EDM requires T violation,
equivalently CP violation by the CPT Theorem.



$$H_{\mu}^{EDM} \stackrel{\beta \rightarrow 0}{\propto} d_{\mu} \bar{\sigma} \cdot \bar{E}$$

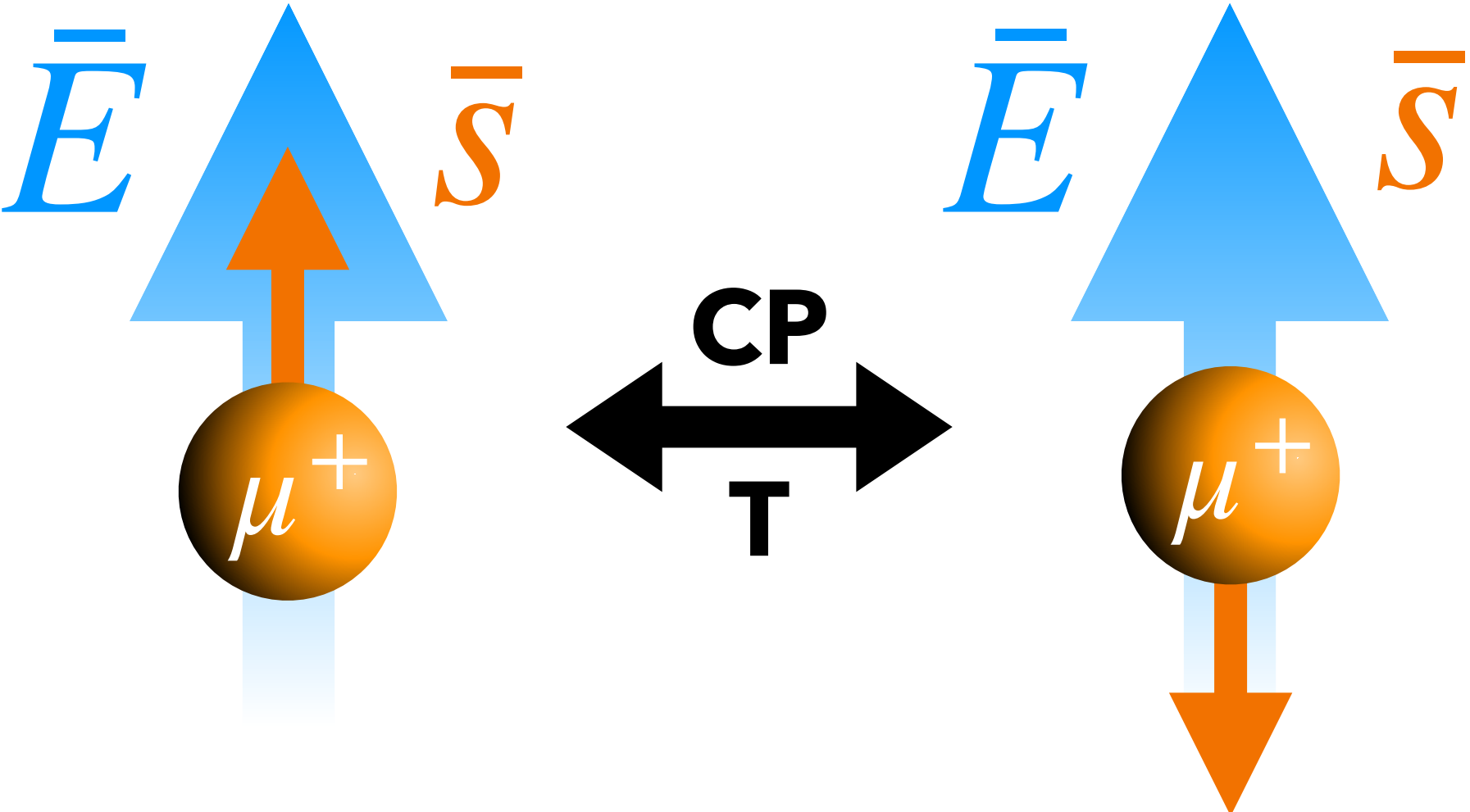
Hamiltonian EDM term is CP violating

SM Prediction: $d_{\mu}^{SM} = 1.4 \times 10^{-38} e \cdot \text{cm}$ (Yamaguchi & Yamanaka, 2020)

$$d_e \leq 1.1 \times 10^{-29} e \cdot \text{cm} \stackrel{LFU}{\implies} d_{\mu} \leq \frac{m_{\mu}}{m_e} d_e = 1.6 \times 10^{-27} e \cdot \text{cm}$$

muEDM Experiment @ PSI

A permanent EDM requires T violation,
equivalently CP violation by the CPT Theorem.



$$H_{\mu}^{EDM} \stackrel{\beta \rightarrow 0}{\propto} d_{\mu} \bar{\sigma} \cdot \bar{E}$$

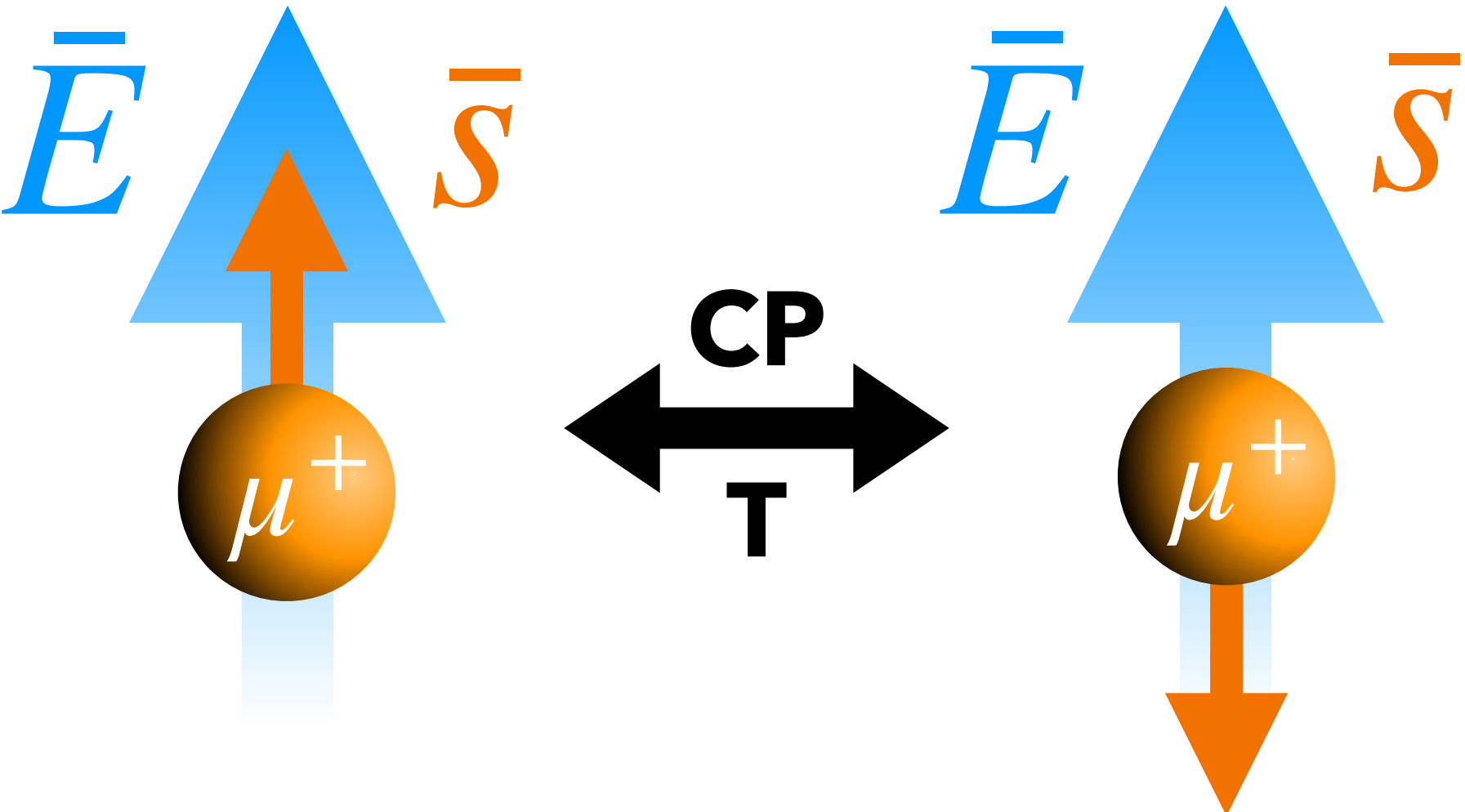
Hamiltonian EDM term is CP violating

SM Prediction: $d_{\mu}^{SM} = 1.4 \times 10^{-38} e \cdot \text{cm}$ (Yamaguchi & Yamanaka, 2020)

$d_e \leq 1.1 \times 10^{-29} e \cdot \text{cm}$ LFU
⇒
? $d_{\mu} \leq \frac{m_{\mu}}{m_e} d_e = 1.6 \times 10^{-27} e \cdot \text{cm}$

muEDM Experiment @ PSI

A permanent EDM requires T violation, equivalently CP violation by the CPT Theorem.



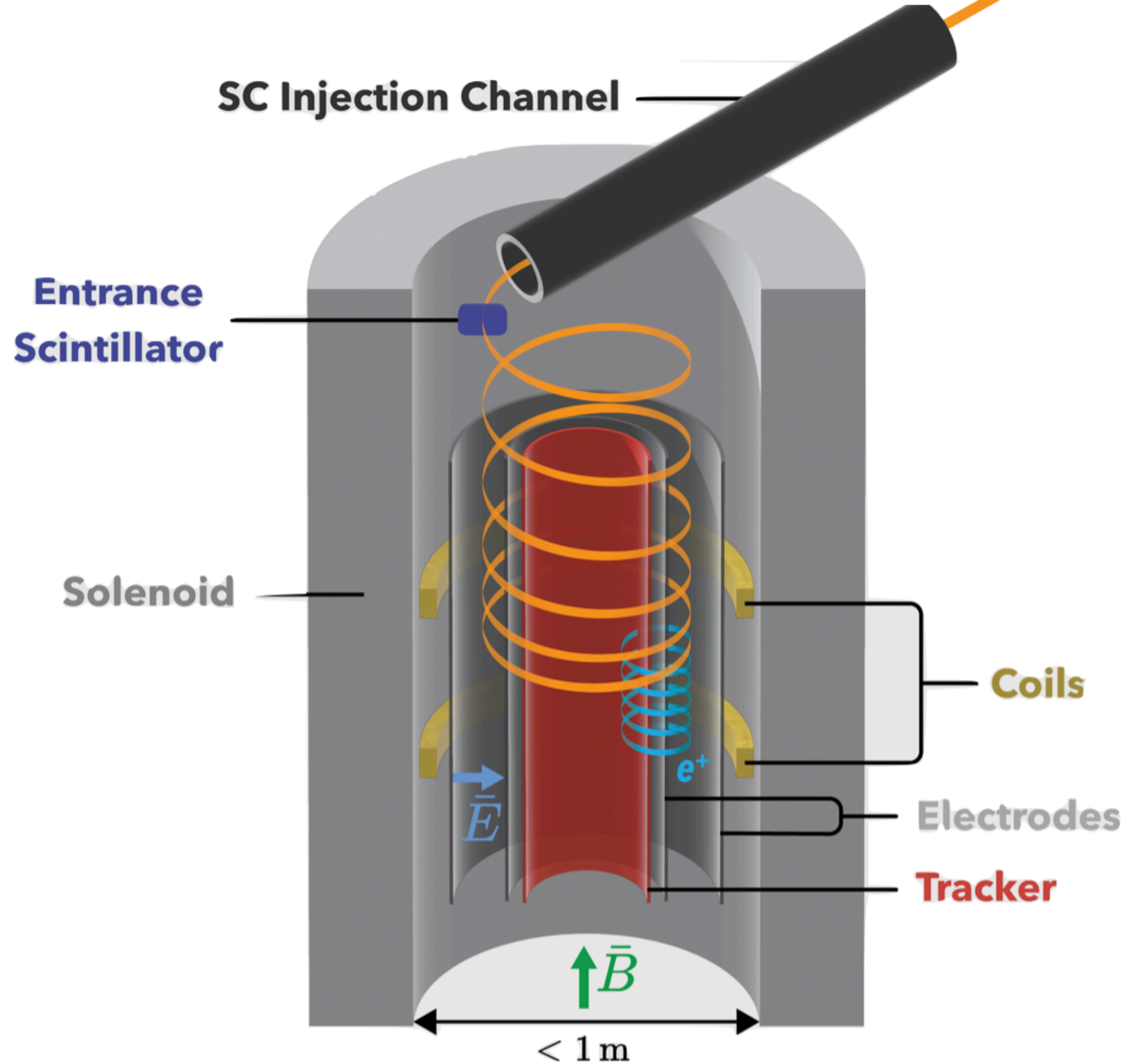
$$H_{\mu}^{EDM} \stackrel{\beta \rightarrow 0}{\propto} d_{\mu} \bar{\sigma} \cdot \bar{E}$$

Hamiltonian EDM term is CP violating

SM Prediction: $d_{\mu}^{SM} = 1.4 \times 10^{-38} e \cdot cm$ (Yamaguchi & Yamanaka, 2020)

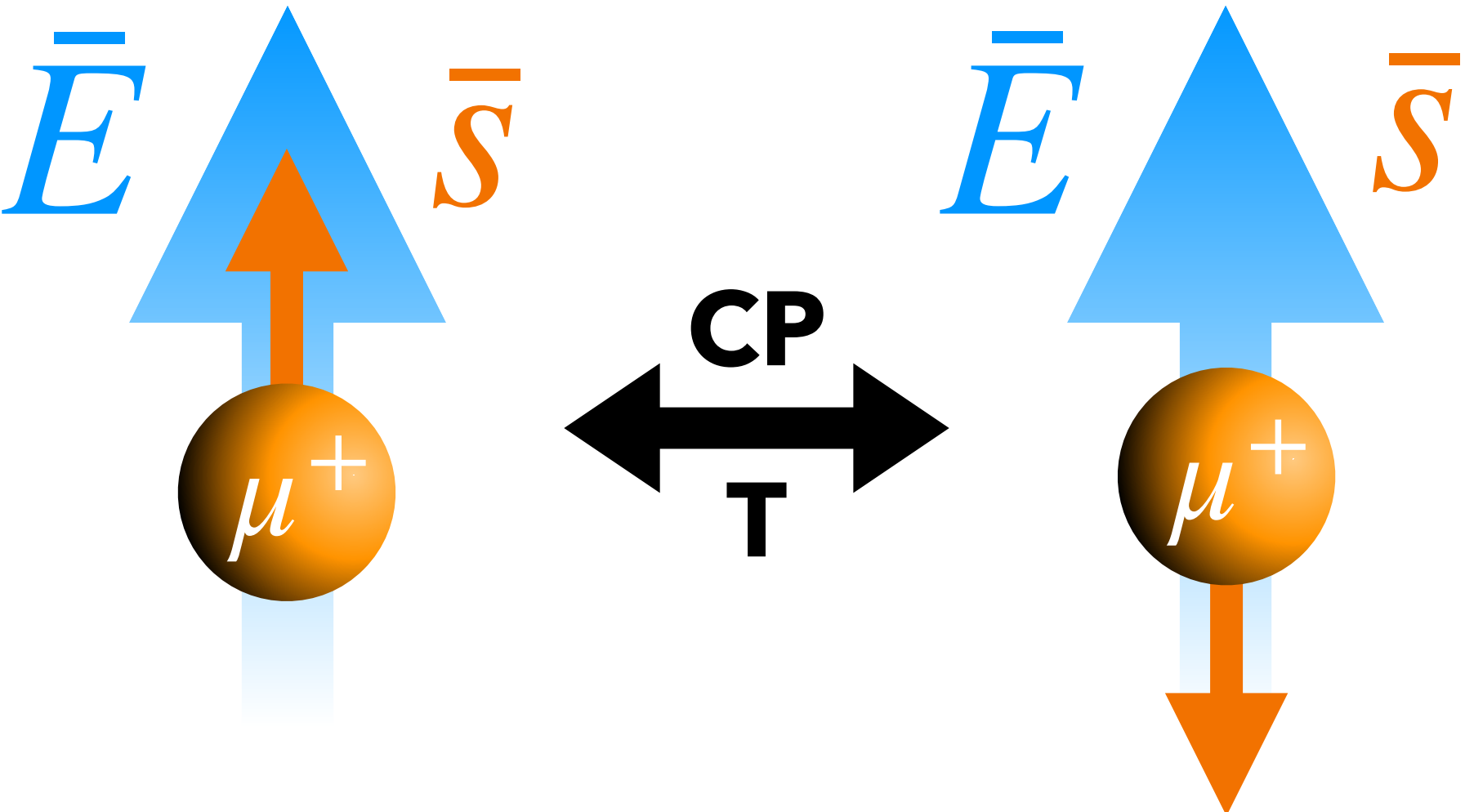
$d_e \leq 1.1 \times 10^{-29} e \cdot cm$ LFU
⇒
? $d_{\mu} \leq \frac{m_{\mu}}{m_e} d_e = 1.6 \times 10^{-27} e \cdot cm$

$\mu^+, 125MeV/c, \mu E1$ Beamline @ PSI



muEDM Experiment @ PSI

A permanent EDM requires T violation, equivalently CP violation by the CPT Theorem.



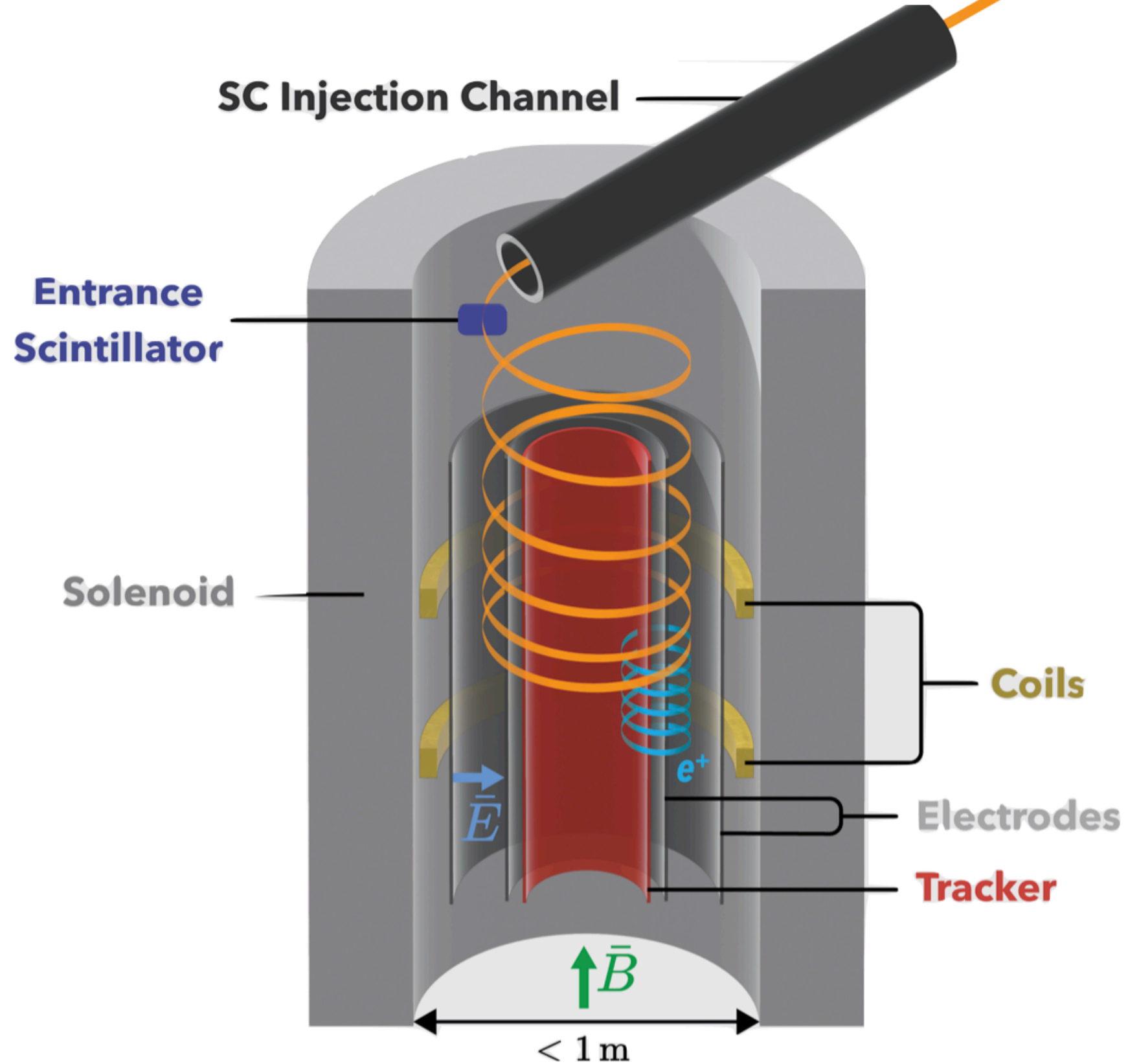
$$H_{\mu}^{EDM} \stackrel{\beta \rightarrow 0}{\propto} d_{\mu} \vec{\sigma} \cdot \vec{E}$$

Hamiltonian EDM term is CP violating

SM Prediction: $d_{\mu}^{SM} = 1.4 \times 10^{-38} e \cdot \text{cm}$ (Yamaguchi & Yamanaka, 2020)

$d_e \leq 1.1 \times 10^{-29} e \cdot \text{cm}$ LFU
⇒
? $d_{\mu} \leq \frac{m_{\mu}}{m_e} d_e = 1.6 \times 10^{-27} e \cdot \text{cm}$

$\mu^+, 125\text{MeV}/c, \mu\text{E1 Beamline @ PSI}$



Final muEDM Experiment Sensitivity

- μE1 Beamline Flux $2 \times 10^8 \mu^+/s$
- Momenta $\gamma = 1.55$
- Polarisation $P_0 \approx 0.95$
- Av. Decay Asymmetry $A \approx 0.3$
- Electric Field $E_f = 2 \text{ MV/m}$

$$\sigma(d_{\mu}) = \frac{a \hbar \gamma}{2 P_0 E_f \sqrt{N} \tau_{\mu} A} \sim 6 \times 10^{-23} e \cdot \text{cm}$$

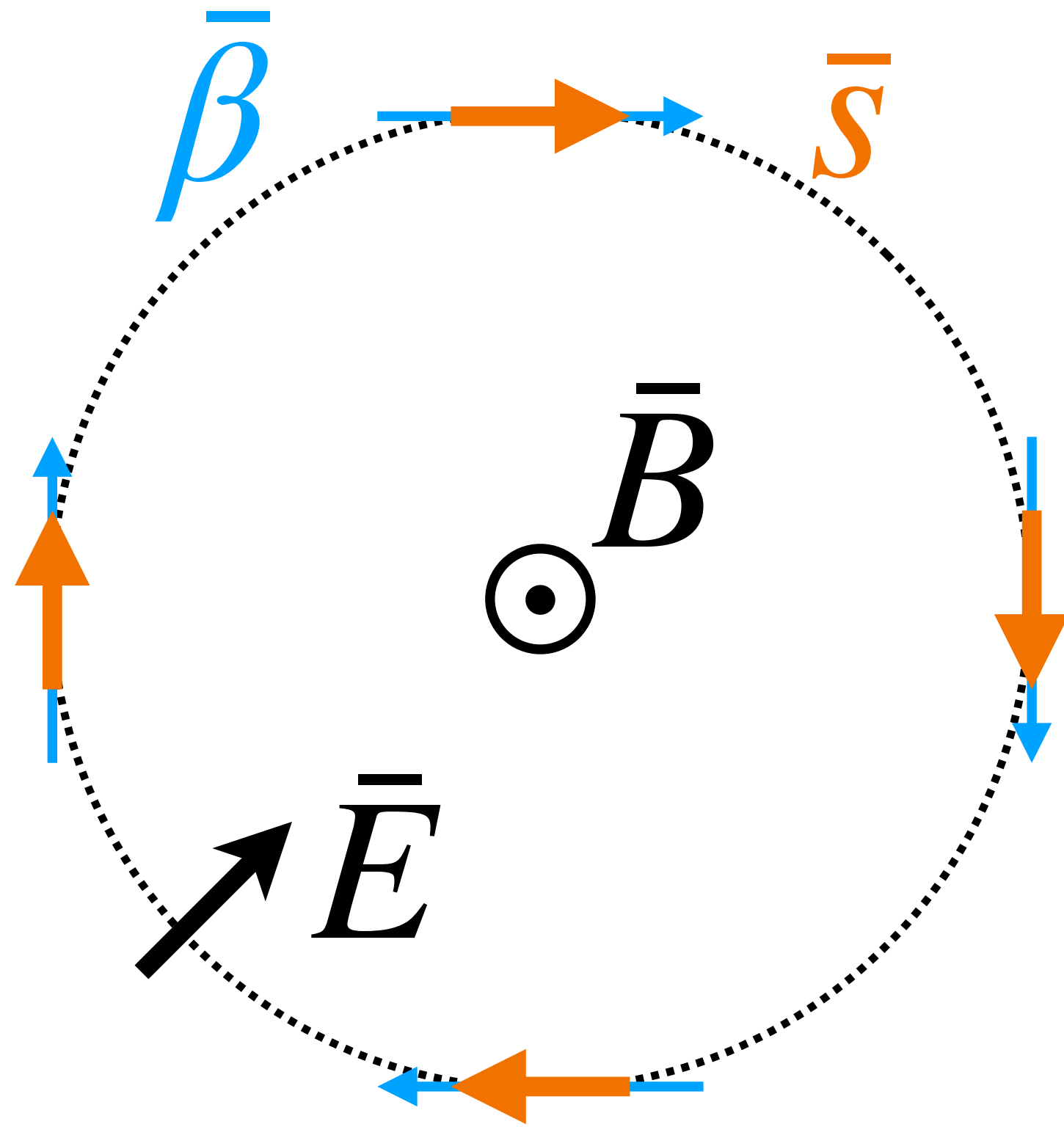
(with $N = 200$ days)

Frozen Spin Technique

Goal: Configure E, B fields such that spin follows velocity vector and EDM is the only inherent source of spin precession.

$$\frac{d\bar{\beta}}{dt} = \bar{\Omega}_c \times \bar{\beta}$$

$$\frac{d\bar{s}}{dt} = \bar{\Omega}_0 \times \bar{s}$$



Frozen Spin Technique

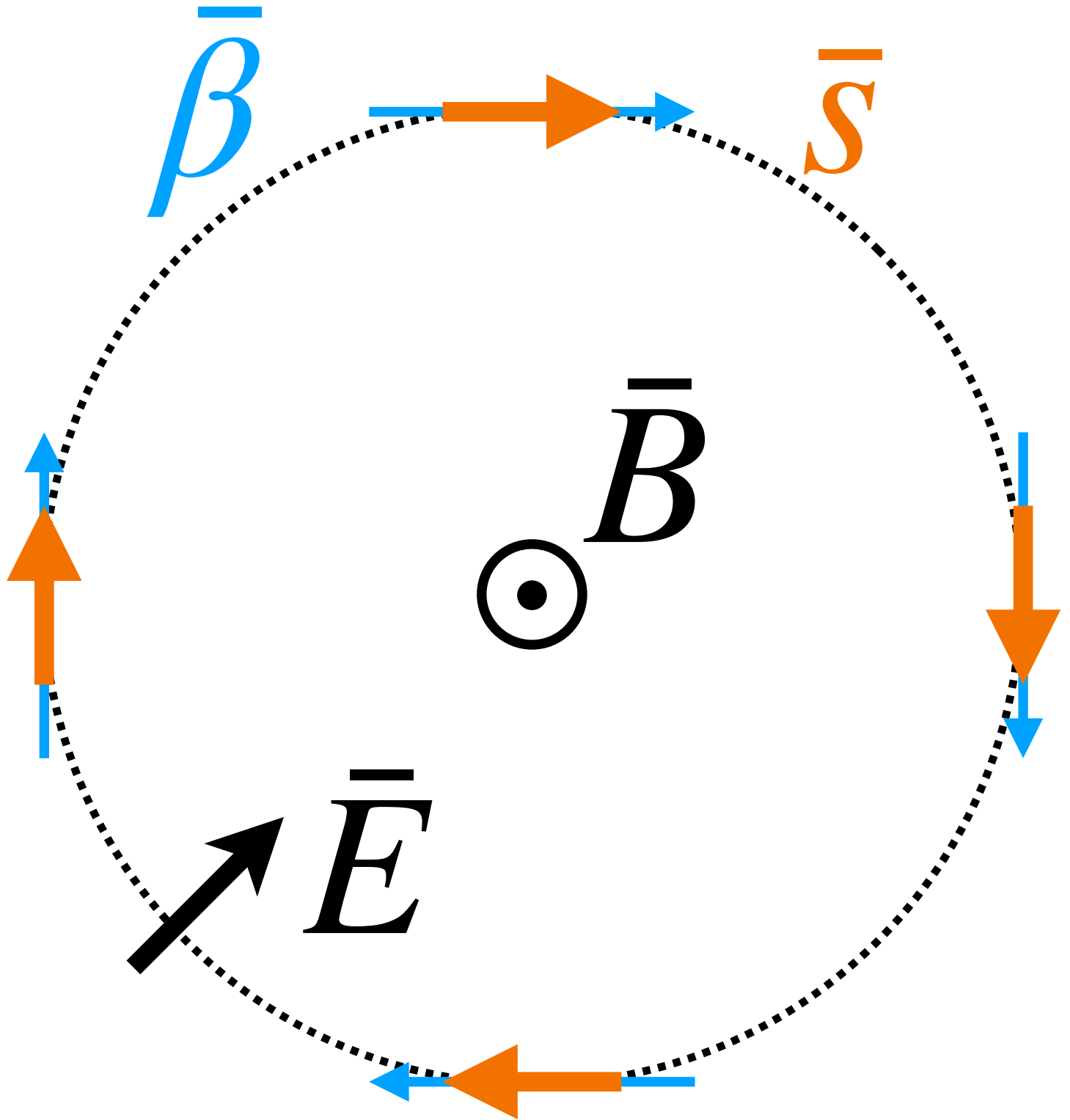
Goal: Configure E, B fields such that spin follows velocity vector and EDM is the only inherent source of spin precession.

$$\frac{d\vec{\beta}}{dt} = \vec{\Omega}_c \times \vec{\beta}$$

$$\frac{d\vec{s}}{dt} = \vec{\Omega}_0 \times \vec{s}$$

$$\vec{\Omega} = \vec{\Omega}_0 - \vec{\Omega}_c = \frac{aq}{m} \left(\vec{B} - \frac{\gamma}{\gamma + 1} (\vec{\beta} \cdot \vec{B}) \vec{\beta} - \left(1 + \frac{1}{a(1 - \gamma^2)} \right) \frac{\vec{\beta} \times \vec{E}}{c} \right)$$

$$+ \frac{\eta q}{2m} \left(\vec{\beta} \times \vec{B} + \frac{\vec{E}}{c} - \frac{\gamma/c}{\gamma + 1} (\vec{\beta} \cdot \vec{E}) \vec{\beta} \right)$$

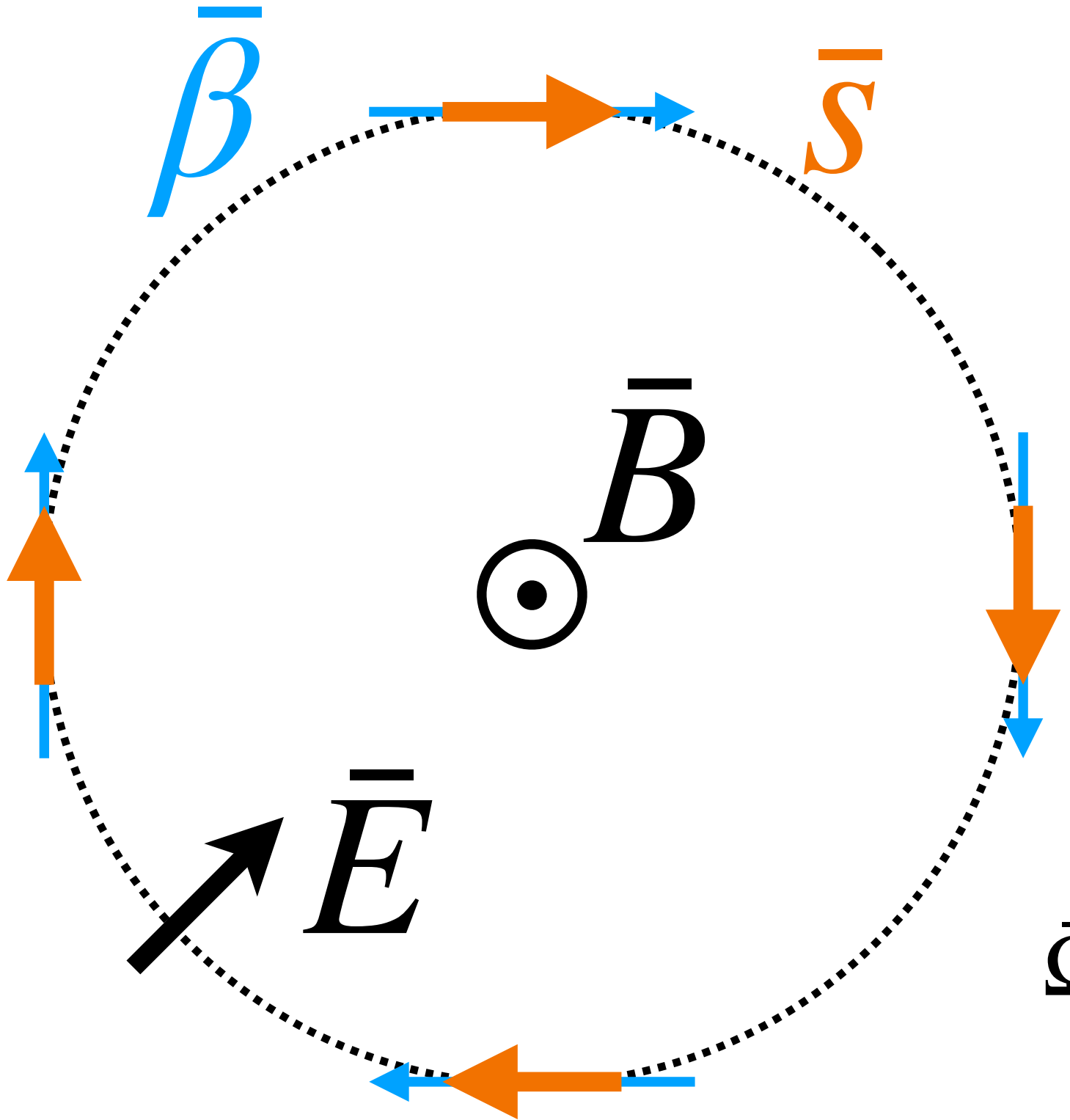


Frozen Spin Technique

Goal: Configure E, B fields such that spin follows velocity vector and EDM is the only inherent source of spin precession.

$$\frac{d\bar{\beta}}{dt} = \bar{\Omega}_c \times \bar{\beta} \quad \frac{d\bar{s}}{dt} = \bar{\Omega}_0 \times \bar{s}$$

$$\bar{\Omega} = \bar{\Omega}_0 - \bar{\Omega}_c = \frac{aq}{m} \left(\bar{B} - \frac{\gamma}{\gamma + 1} (\bar{\beta} \cdot \bar{B}) \bar{\beta} - \left(1 + \frac{1}{a(1 - \gamma^2)} \right) \frac{\bar{\beta} \times \bar{E}}{c} \right)$$



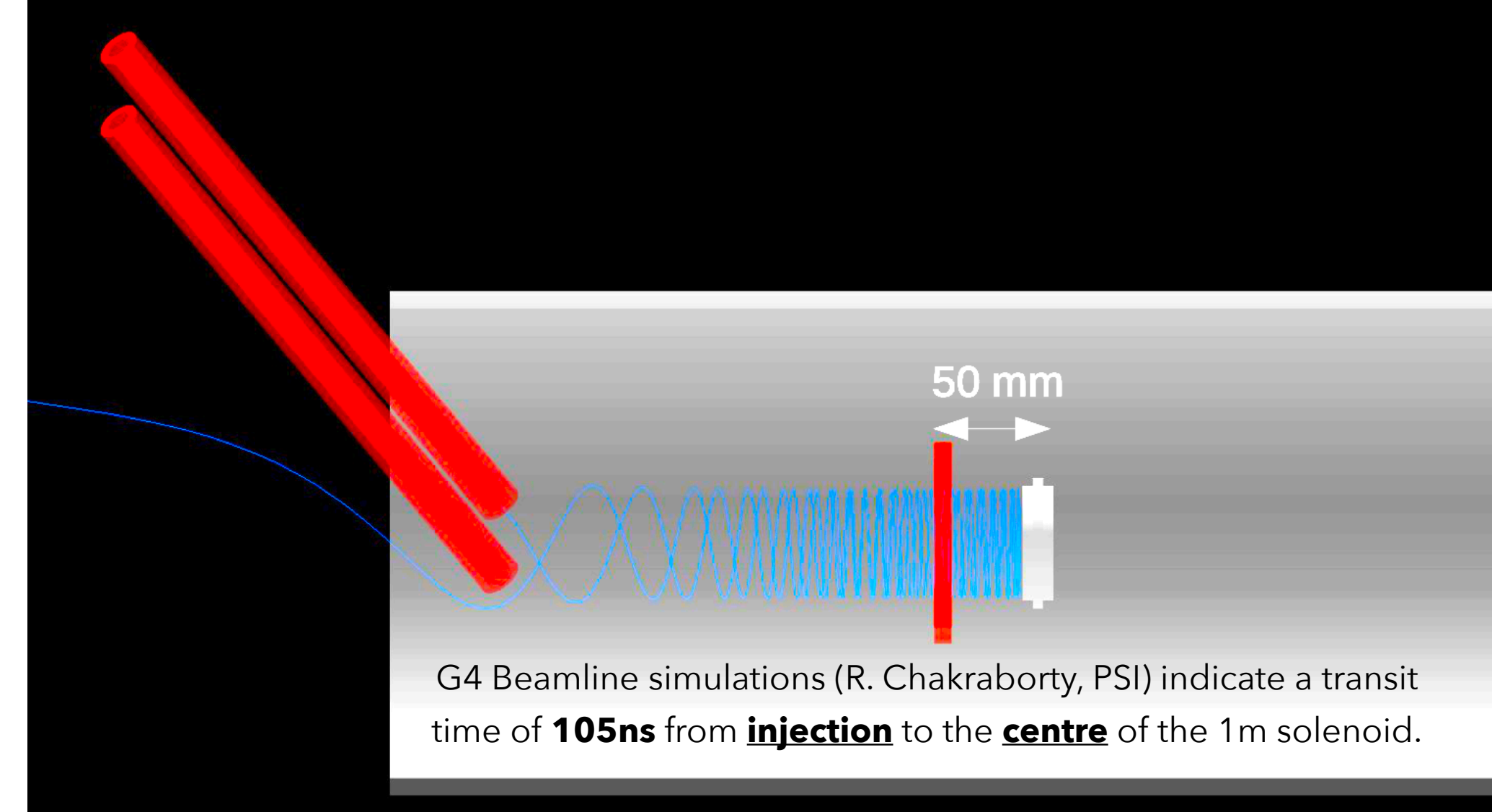
$$+ \frac{\eta q}{2m} \left(\bar{\beta} \times \bar{B} + \frac{\bar{E}}{c} - \frac{\gamma/c}{\gamma + 1} (\bar{\beta} \cdot \bar{E}) \bar{\beta} \right)$$

Frozen Spin Condition : $E_f \overset{a \ll 1}{\approx} aB\beta c\gamma^2$

$$\bar{\Omega} = \frac{\eta q}{2m} \left(\bar{\beta} \times \bar{B} - \frac{\bar{E}}{c} \right) \quad \text{for } |\bar{E}| = E_f, \quad \bar{\beta} \cdot \bar{E} = \bar{\beta} \cdot \bar{B} = \bar{E} \cdot \bar{B} = 0$$

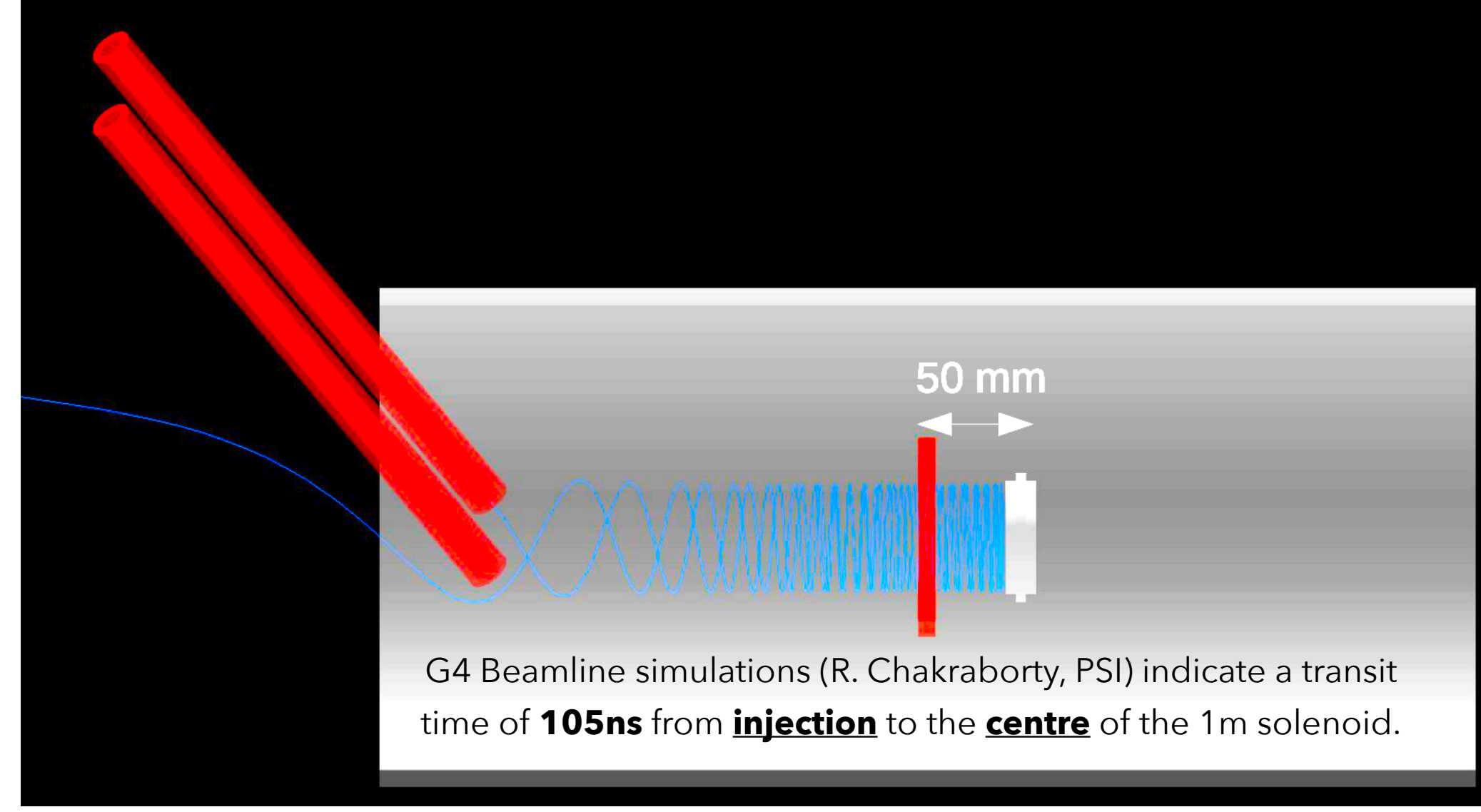
Magnetic Kick Specifications

- **Objective:** achieve stable circular orbit by kicking longitudinal momentum into the transverse plane when muon enters weakly focusing storage region.
- **Challenge:** the muon transit time to the storage region is $\sim 100\text{ns}$ after a trigger is generated at the entrance detector.
- **Technical Problem:** High amplitude, short duration pulsed magnetic field must be rapidly triggered, with strong tail suppression.

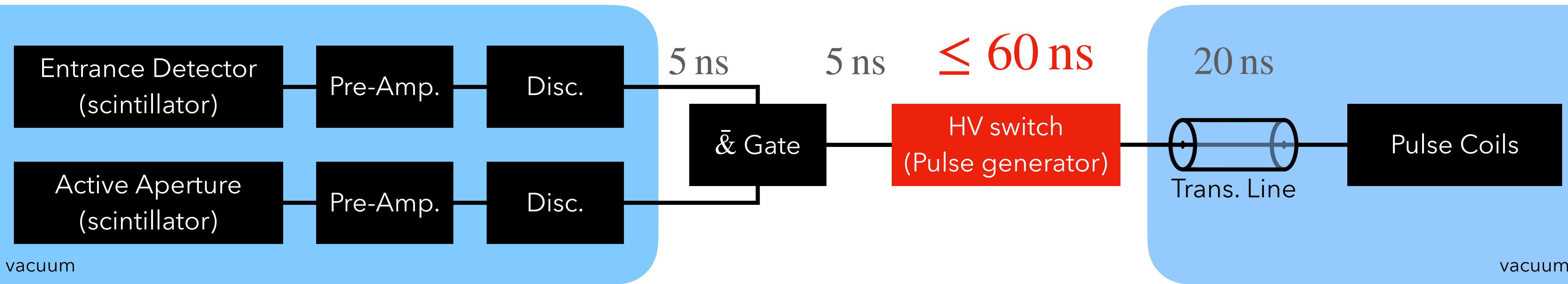


Magnetic Kick Specifications

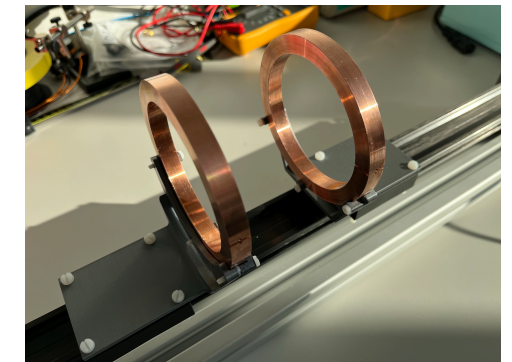
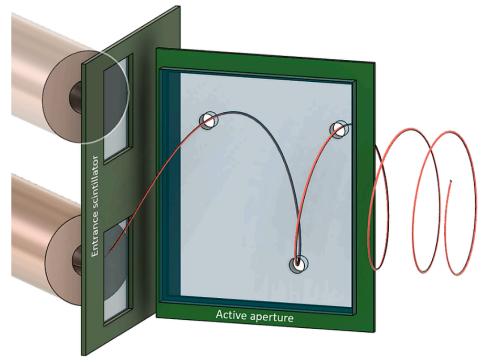
- **Objective:** achieve stable circular orbit by kicking longitudinal momentum into the transverse plane when muon enters weakly focusing storage region.
- **Challenge:** the muon transit time to the storage region is $\sim 100\text{ns}$ after a trigger is generated at the entrance detector.
- **Technical Problem:** High amplitude, short duration pulsed magnetic field must be rapidly triggered, with strong tail suppression.



15 ns

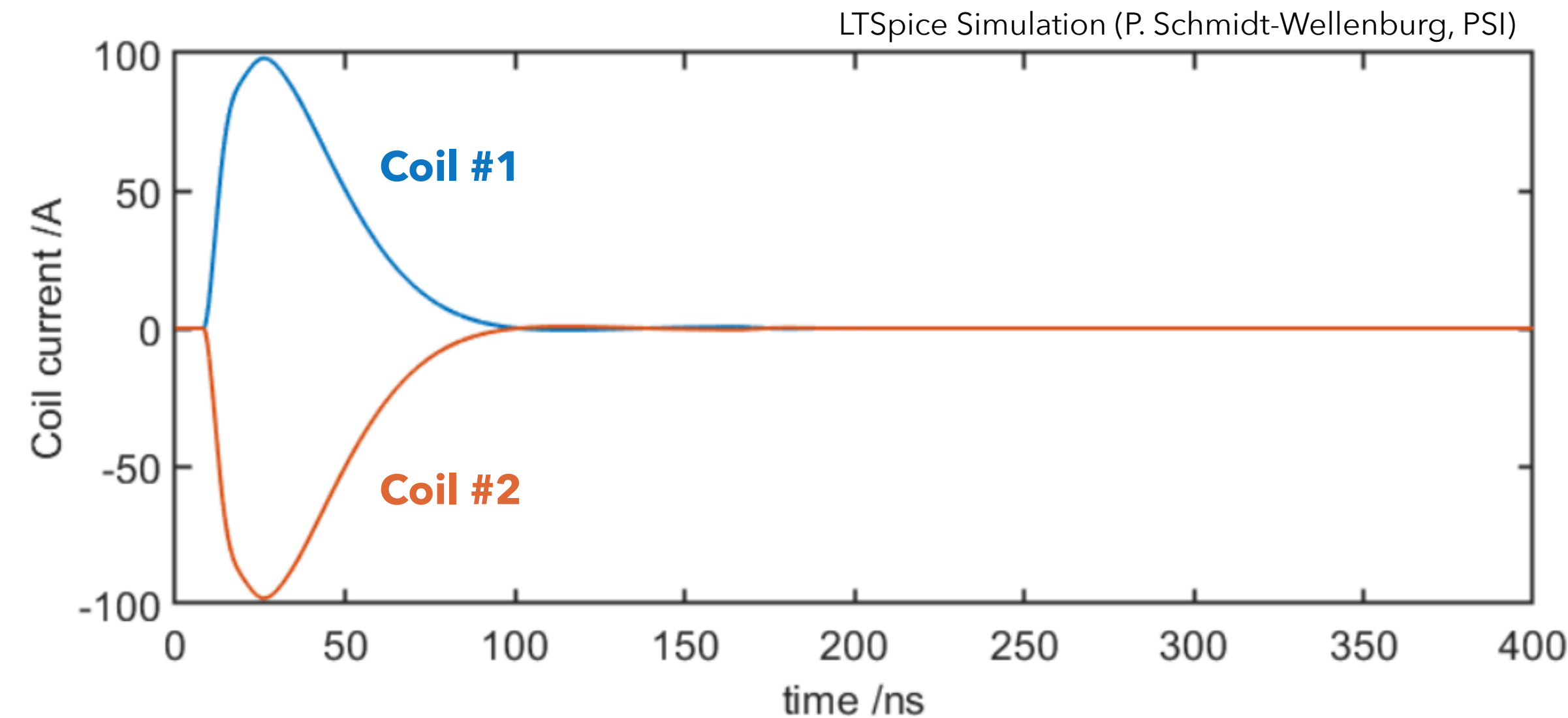


Assuming time of 100ns for PSC magnet, the delays in the lines constrain the HV switching of the pulse generator to be $<60\text{ns}$.



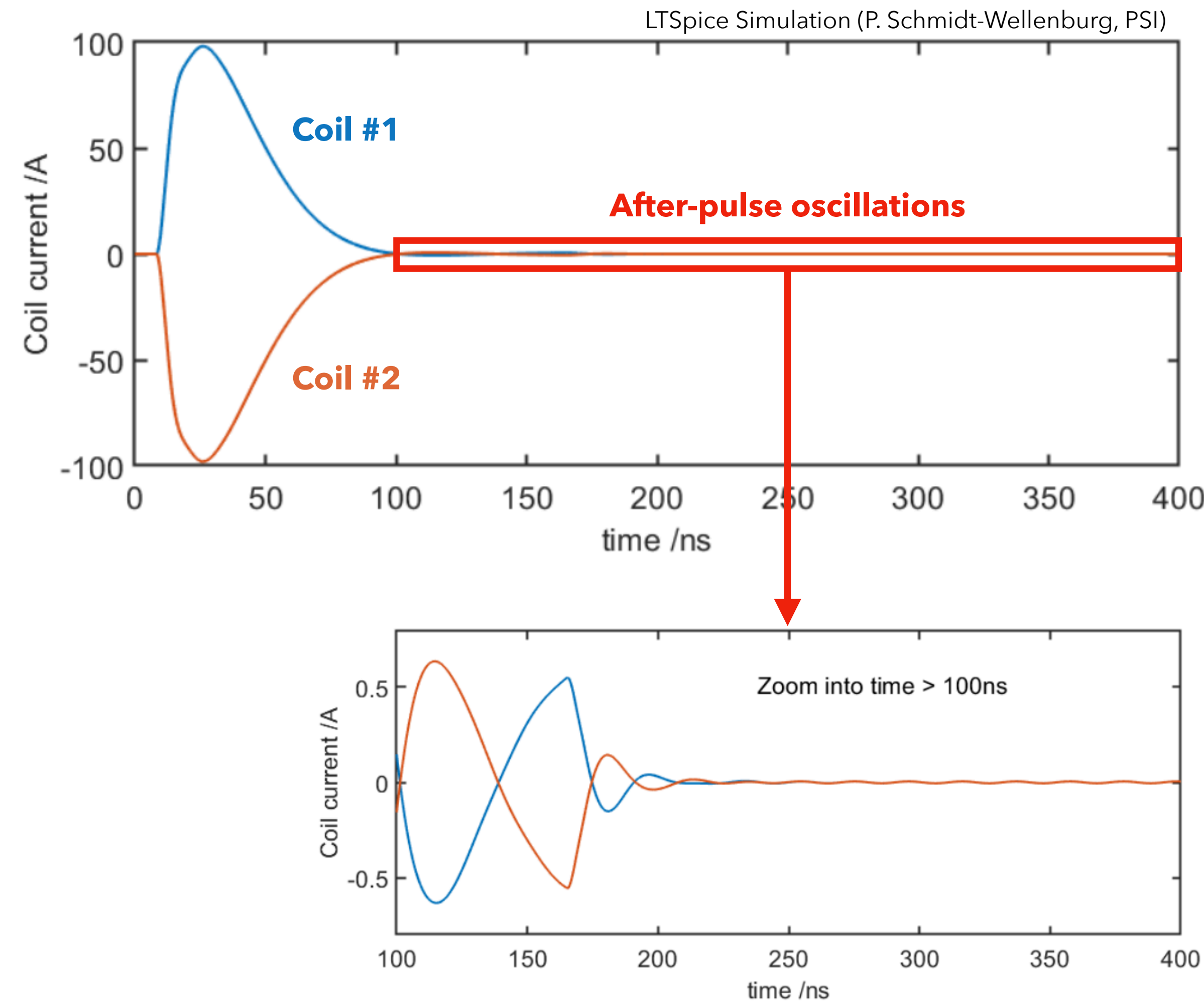
Current Pulse Specifications

- Delay between trigger input and pulse output $\Delta t_d < 60$ ns
- Pulse FWHM ~ 40 ns
- Peak current ~ 170 A
- Eddy current damping by electrodes, need safety factor in peak current of at least a factor ~ 1.5
- Suppression of current oscillations in tail to < 1 A (corresponding to radial magnetic field $< 5 \mu\text{T}$)



Current Pulse Specifications

- Delay between trigger input and pulse output $\Delta t_d < 60$ ns
- Pulse FWHM ~ 40 ns
- Peak current ~ 170 A
- Eddy current damping by electrodes, need safety factor in peak current of at least a factor ~ 1.5
- Suppression of current oscillations in tail to < 1 A (corresponding to radial magnetic field $< 5 \mu\text{T}$)

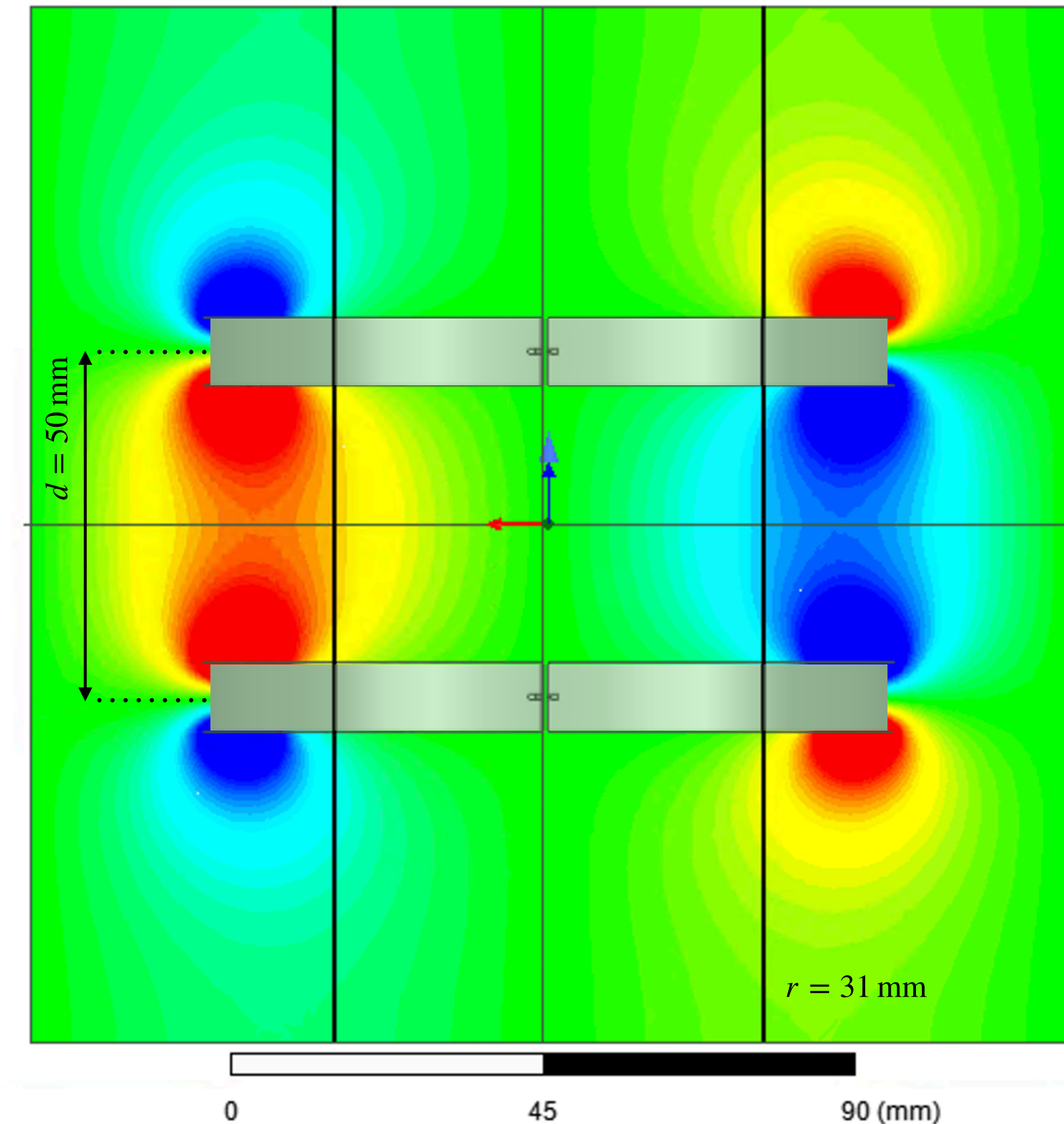


Pulse Coils

- Need low inductance to drive high-frequency, high-current pulse and minimise residual oscillations.
- Self inductance of each coil:
 - Measured: $L = 121 \pm 1$ nH
 - Wire Loop Approximation: $L = 129$ nH
 - Ansys FEM: $L = 139$ nH
- Optimisation of coil geometry to be informed by simulation studies of muon injection.

Radial Projection of B Field

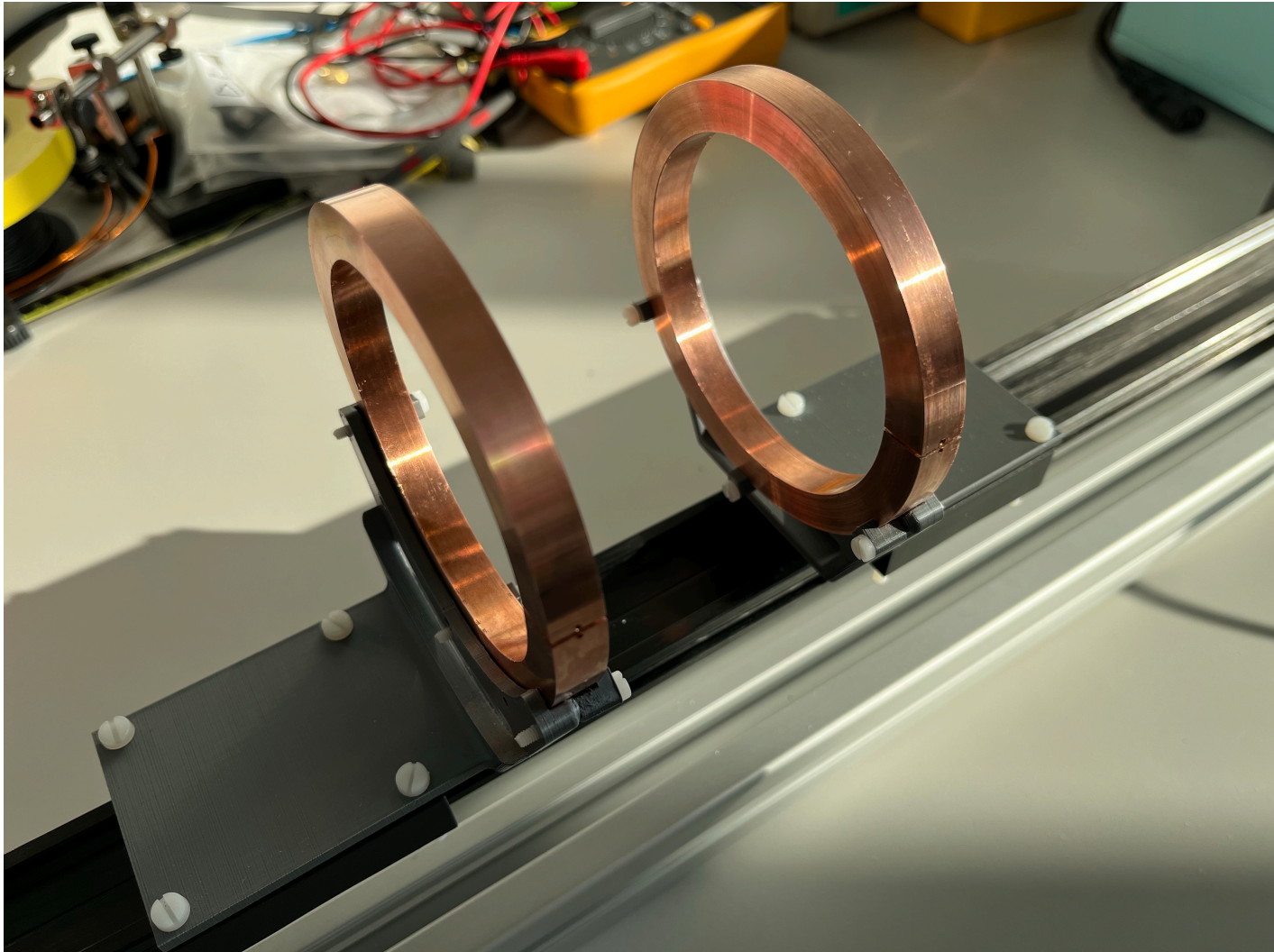
$$\vec{B}(t) \cdot \hat{s}_{mu}(t)$$

$\hat{s}_{mu}(t)$ = radial coordinate of muon path in cylindrical coordinate system.
The B field radial projection thus kicks the longitudinal momentum.

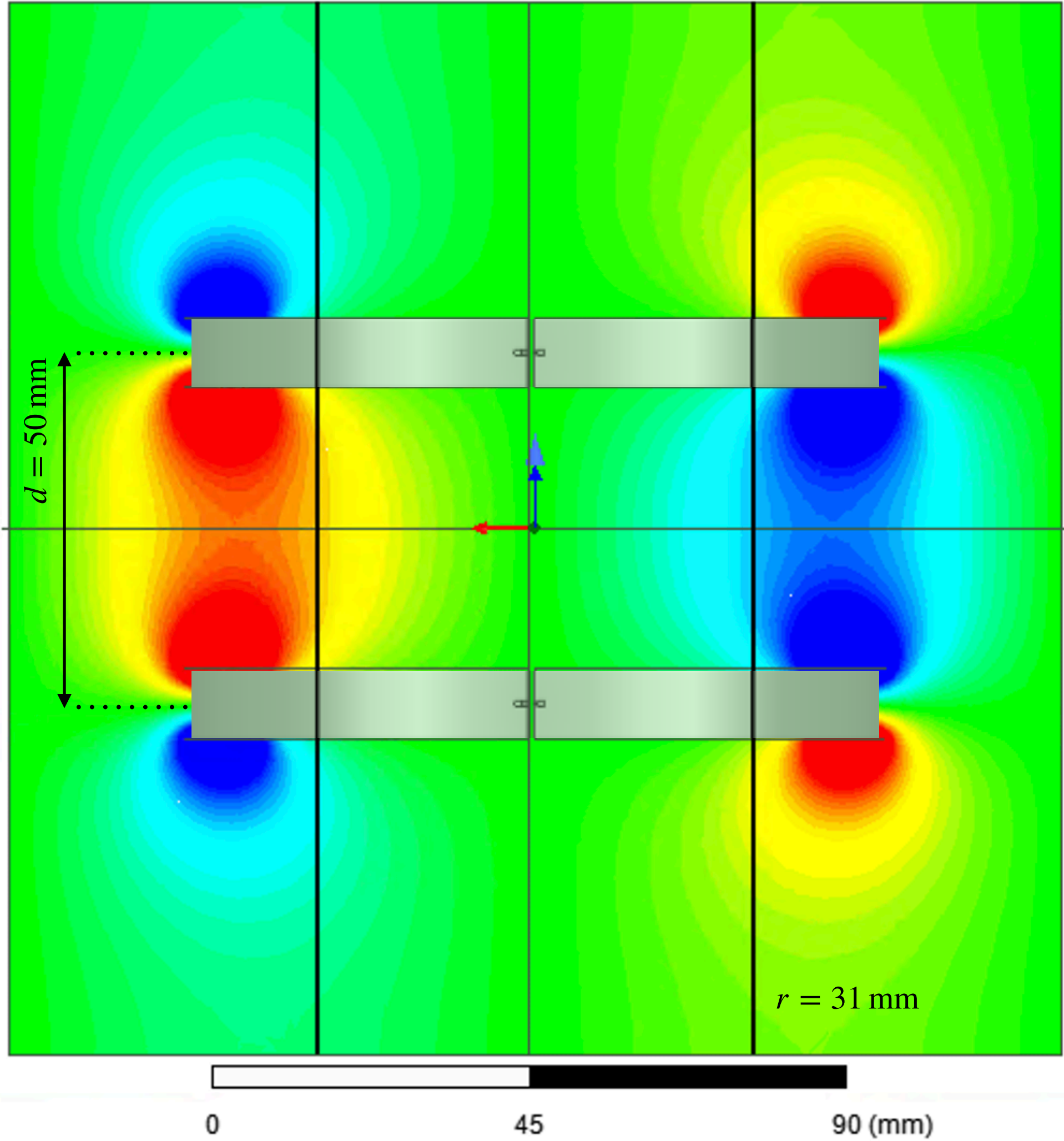
Pulse Coils

- Need low inductance to drive high-frequency, high-current pulse and minimise residual oscillations.
- Self inductance of each coil:
 - Measured: $L = 121 \pm 1 \text{ nH}$
 - Wire Loop Approximation: $L = 129 \text{ nH}$
 - Ansys FEM: $L = 139 \text{ nH}$
- Optimisation of coil geometry to be informed by simulation studies of muon injection.



Radial Projection of B Field

$\vec{B}(t) \cdot \hat{s}_{mu}(t)$ -15 $\mu\text{T/A}$ 0 15 $\mu\text{T/A}$

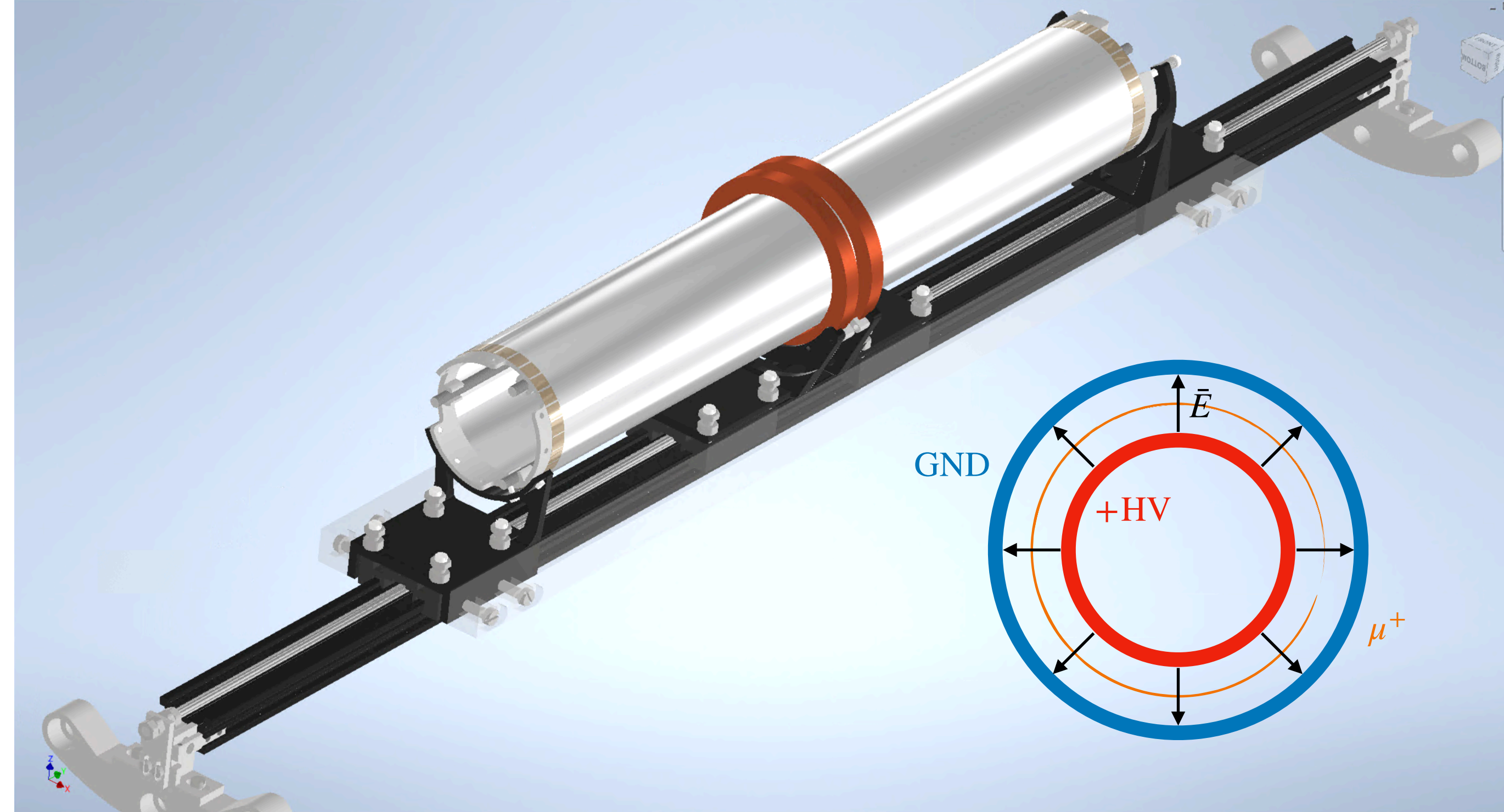


$\hat{s}_{mu}(t)$ = radial coordinate of muon path in cylindrical coordinate system.
The B field radial projection thus kicks the longitudinal momentum.

Thin Foil Electrodes

Requirements

- Precise alignment (systematic effects)
 - *Material robust as thin foil*
- Eddy currents
 - *Low electrical conductivity*
 - *Weak thermal expansion*
 - *High thermal conductivity*
- Material budget
 - *Weak multiple scattering of positrons*



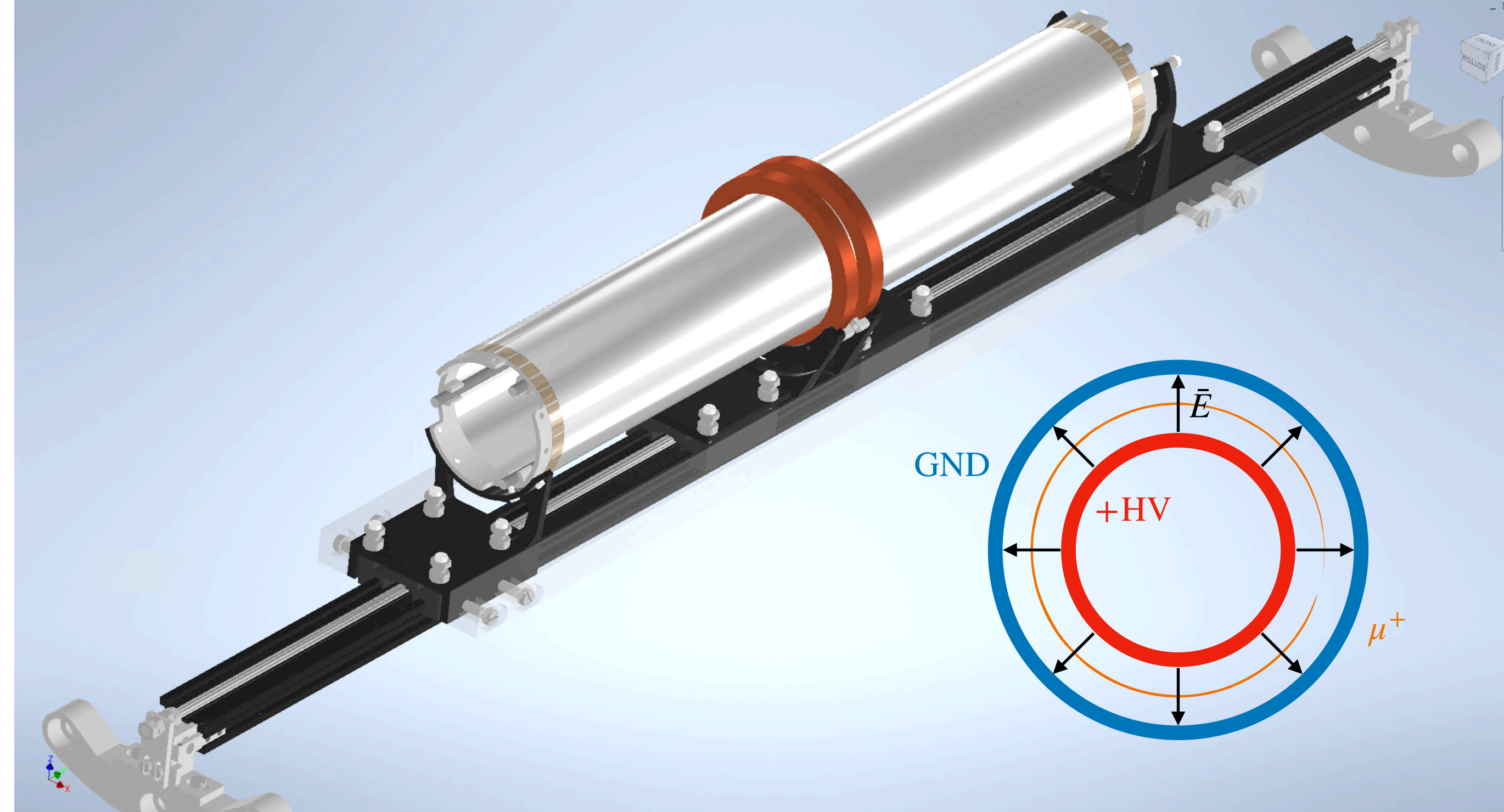
Thin Foil Electrodes

Requirements

- Precise alignment (systematic effects)
 - *Material robust as thin foil*
- Eddy currents
 - *Low electrical conductivity*
 - *Weak thermal expansion*
 - *High thermal conductivity*
- Material budget
 - *Weak multiple scattering of positrons*

Candidates

- Aluminised polymer (eg. Mylar, Kapton)
 - Advantages: aluminium can be very thin ($\sim 20\text{nm}$), robust
 - Disadvantages: high thermal expansion, high conductivity
- Graphite
 - Advantage: low conductivity
 - Disadvantage: poor mechanical robustness



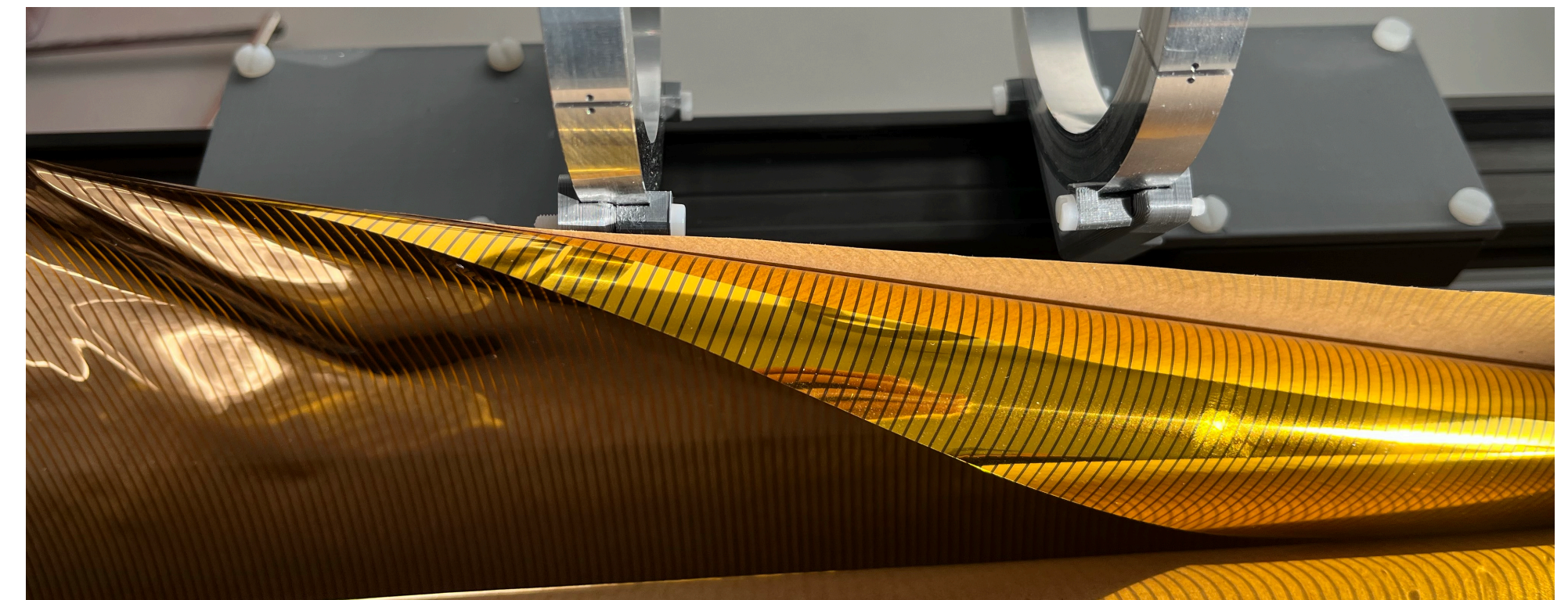
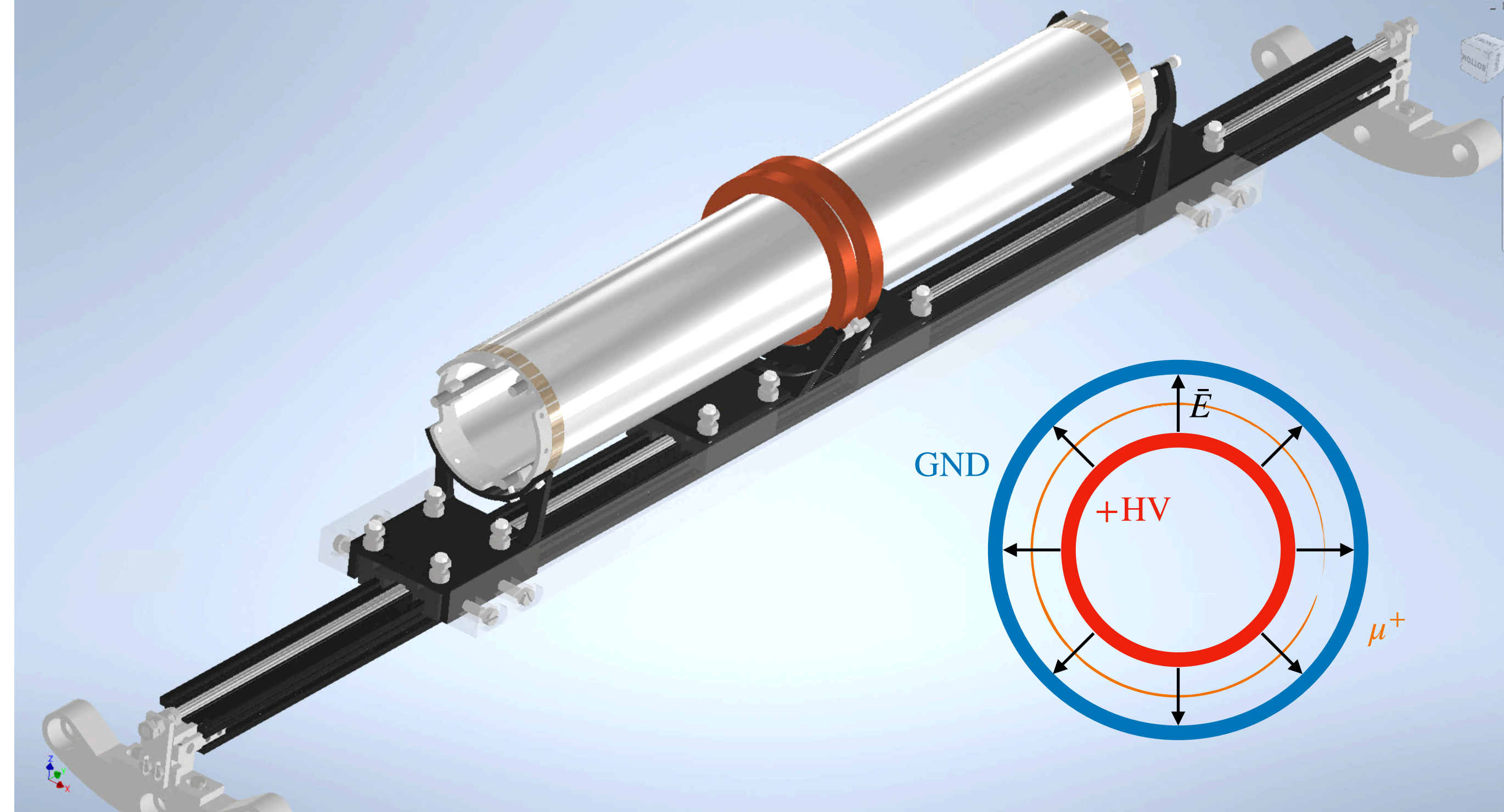
Thin Foil Electrodes

Requirements

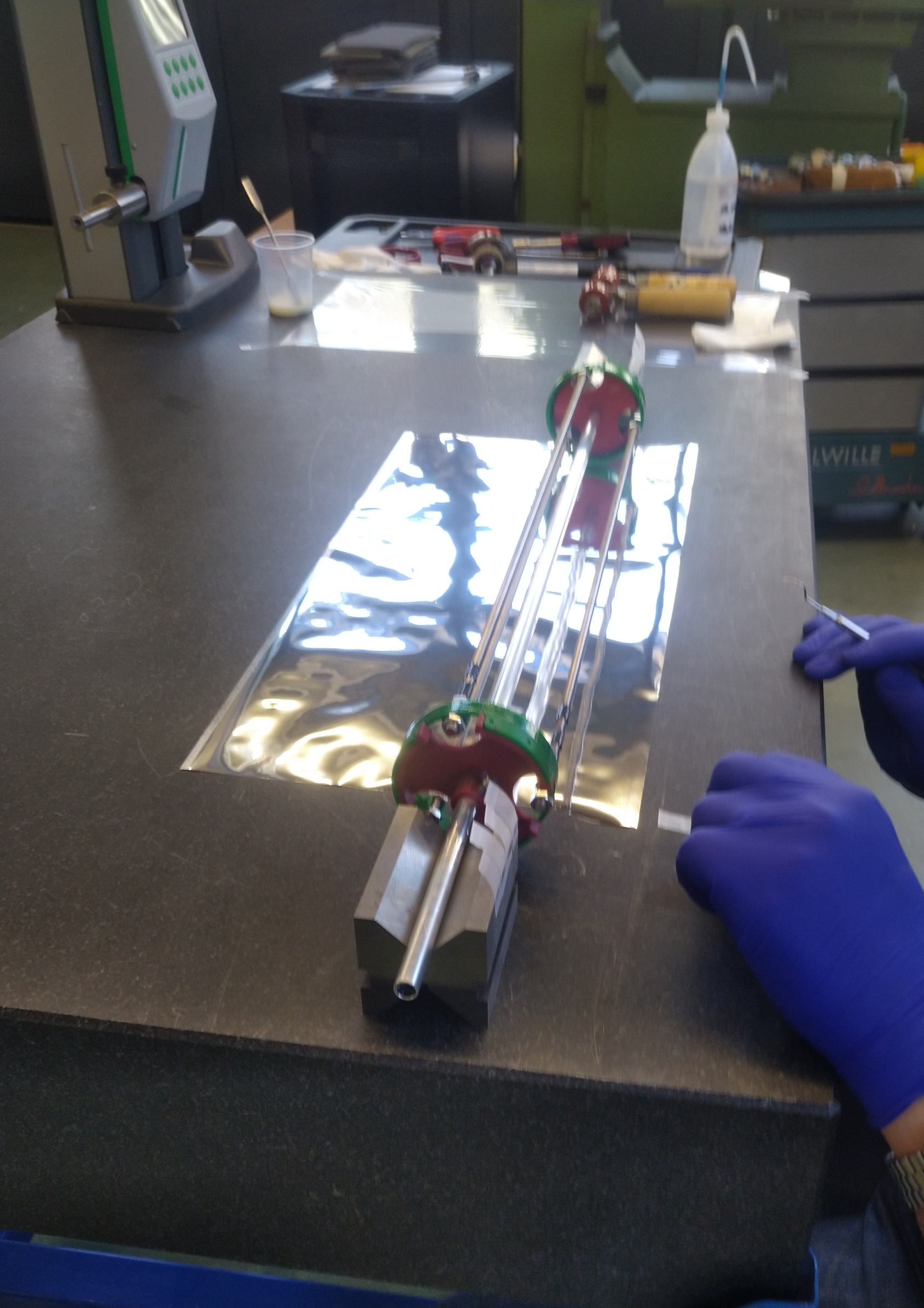
- Precise alignment (systematic effects)
 - *Material robust as thin foil*
- Eddy currents
 - *Low electrical conductivity*
 - *Weak thermal expansion*
 - *High thermal conductivity*
- Material budget
 - *Weak multiple scattering of positrons*

Candidates

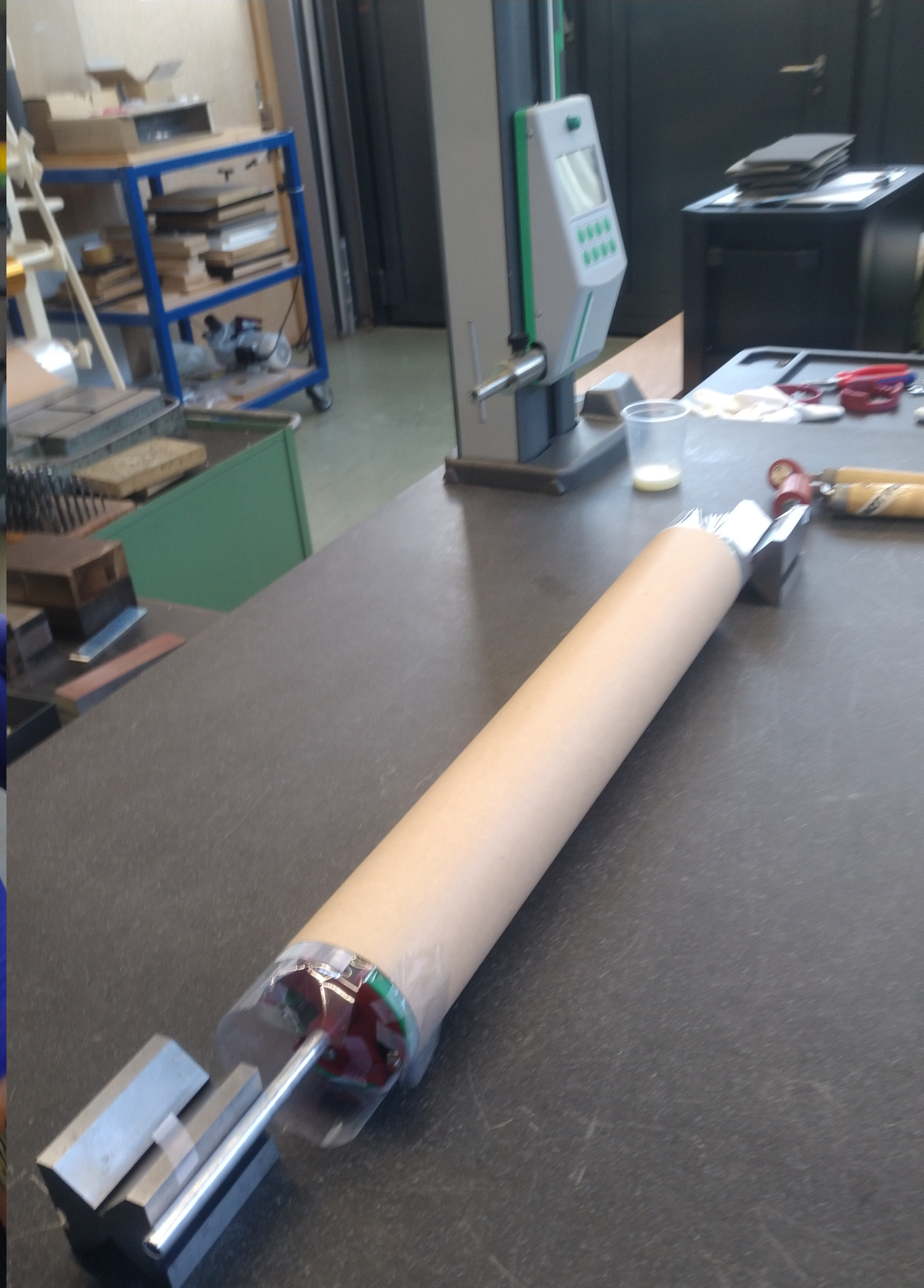
- Aluminised polymer (eg. Mylar, Kapton)
 - Advantages: aluminium can be very thin ($\sim 20\text{nm}$), robust
 - Disadvantages: high thermal expansion, high conductivity
- Graphite
 - Advantage: low conductivity
 - Disadvantage: poor mechanical robustness



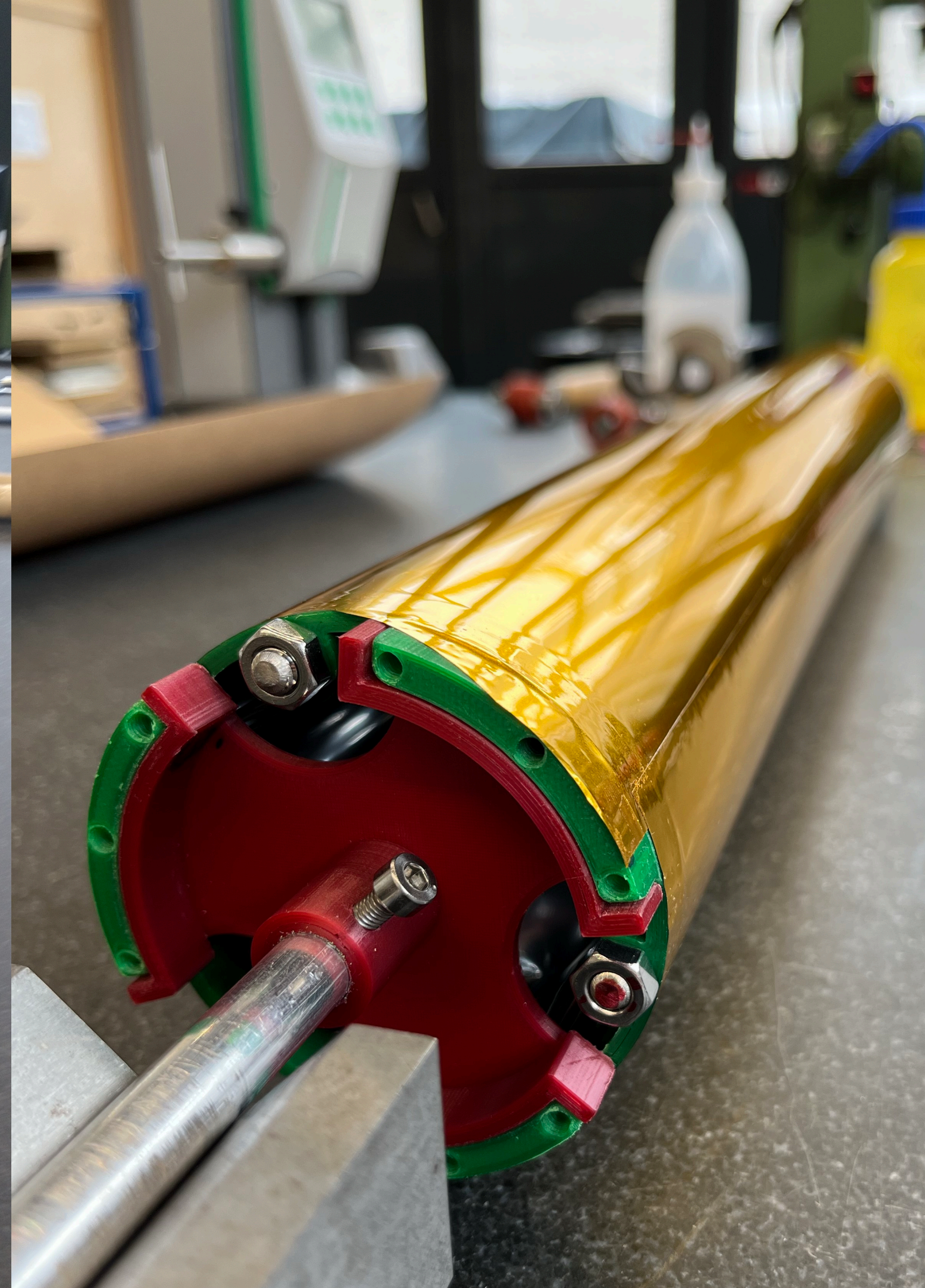
New prototypes under development using aluminised Kapton with 2mm stripes (2.2mm pitch) to suppress radial eddy currents.



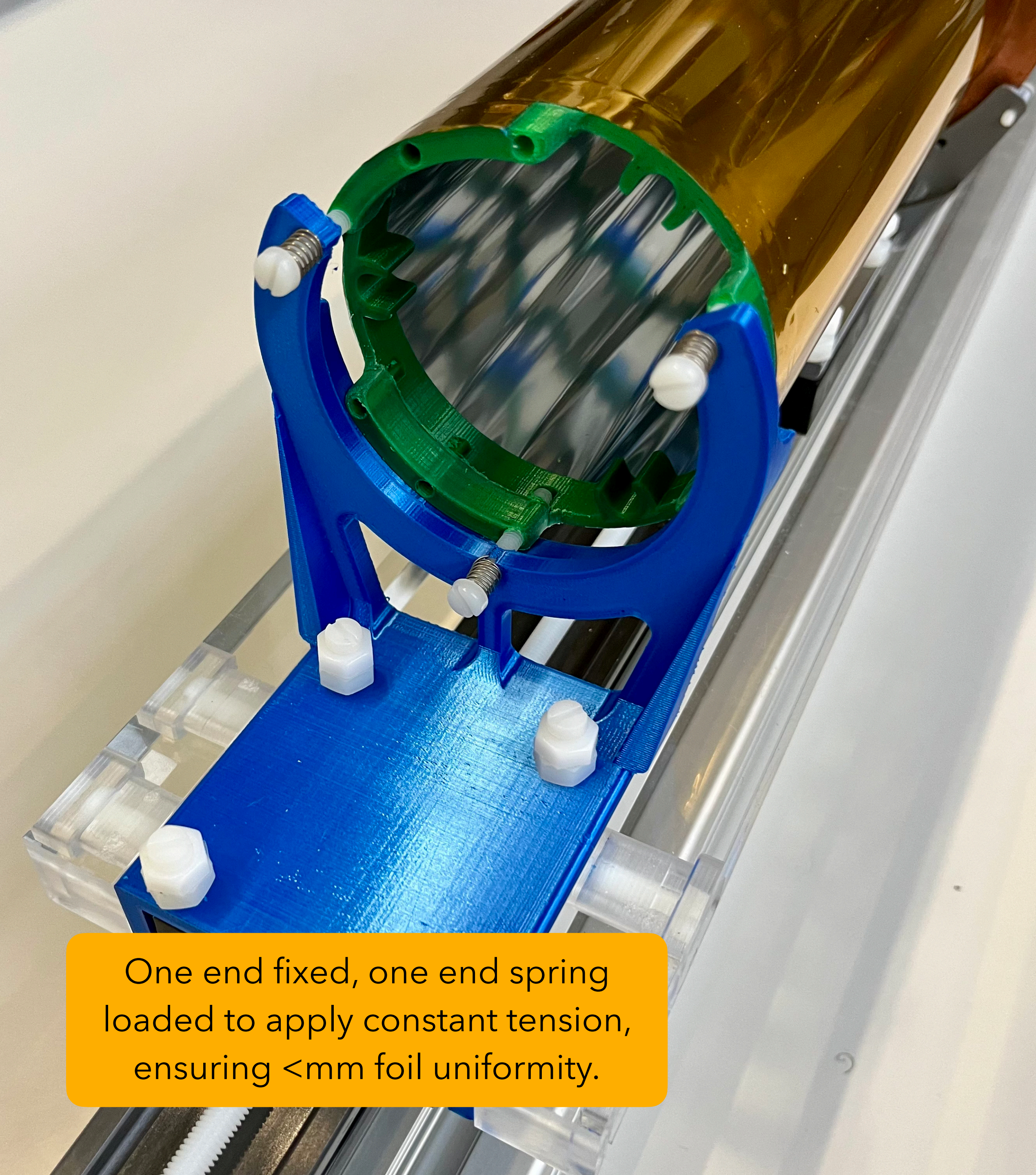
Foil is cut to size, and end rings are fixed and aligned using threaded steel rods.



Foil is rotated and glued onto the end rings, and wrapped tightly until epoxy glue is set.



Structurally fixed cylinder, ready to mount onto electrode supports.



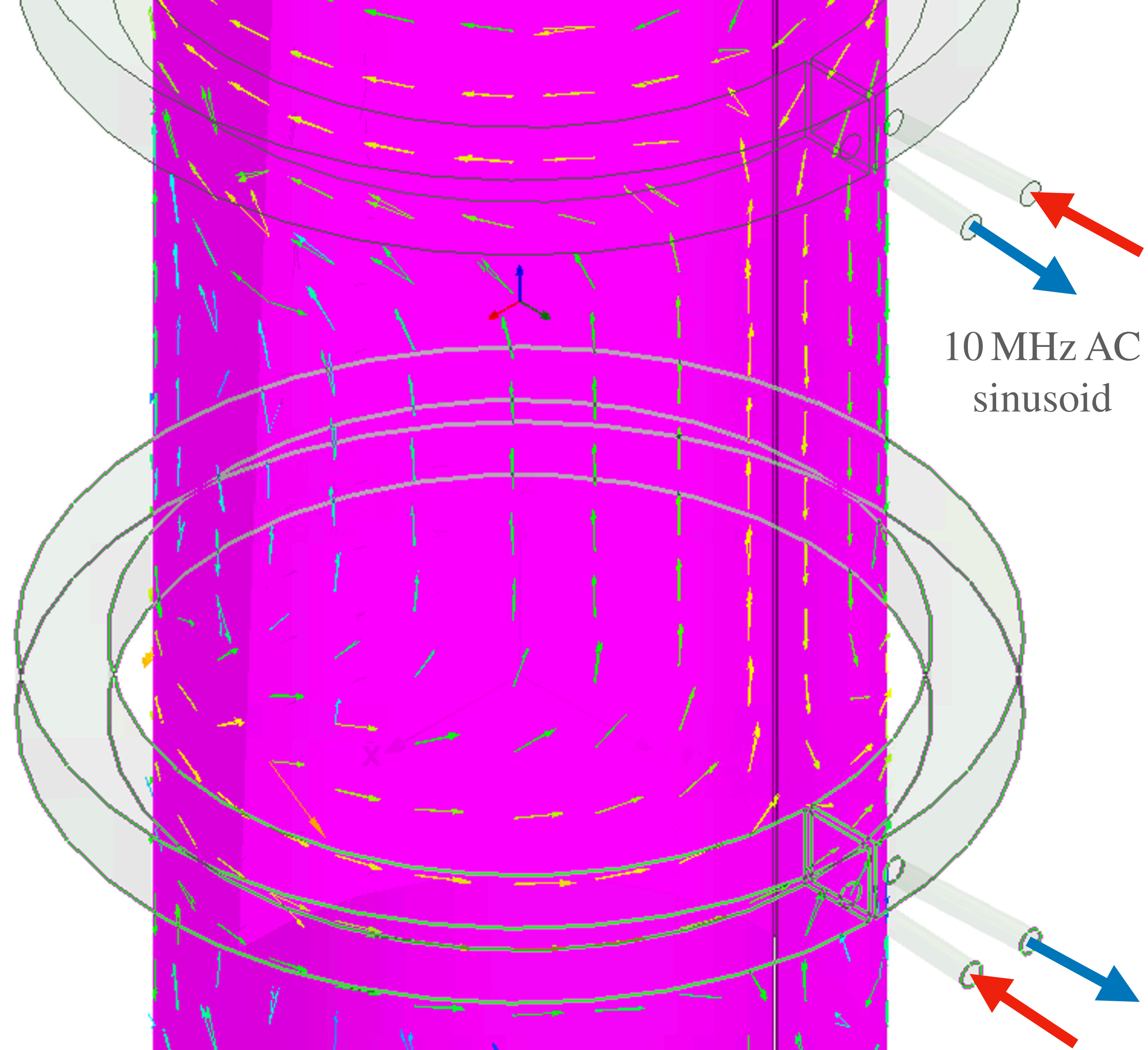
One end fixed, one end spring loaded to apply constant tension, ensuring $< \text{mm}$ foil uniformity.



Material budget of internal (HV) electrode likely less important than for the outer (GND) electrode.

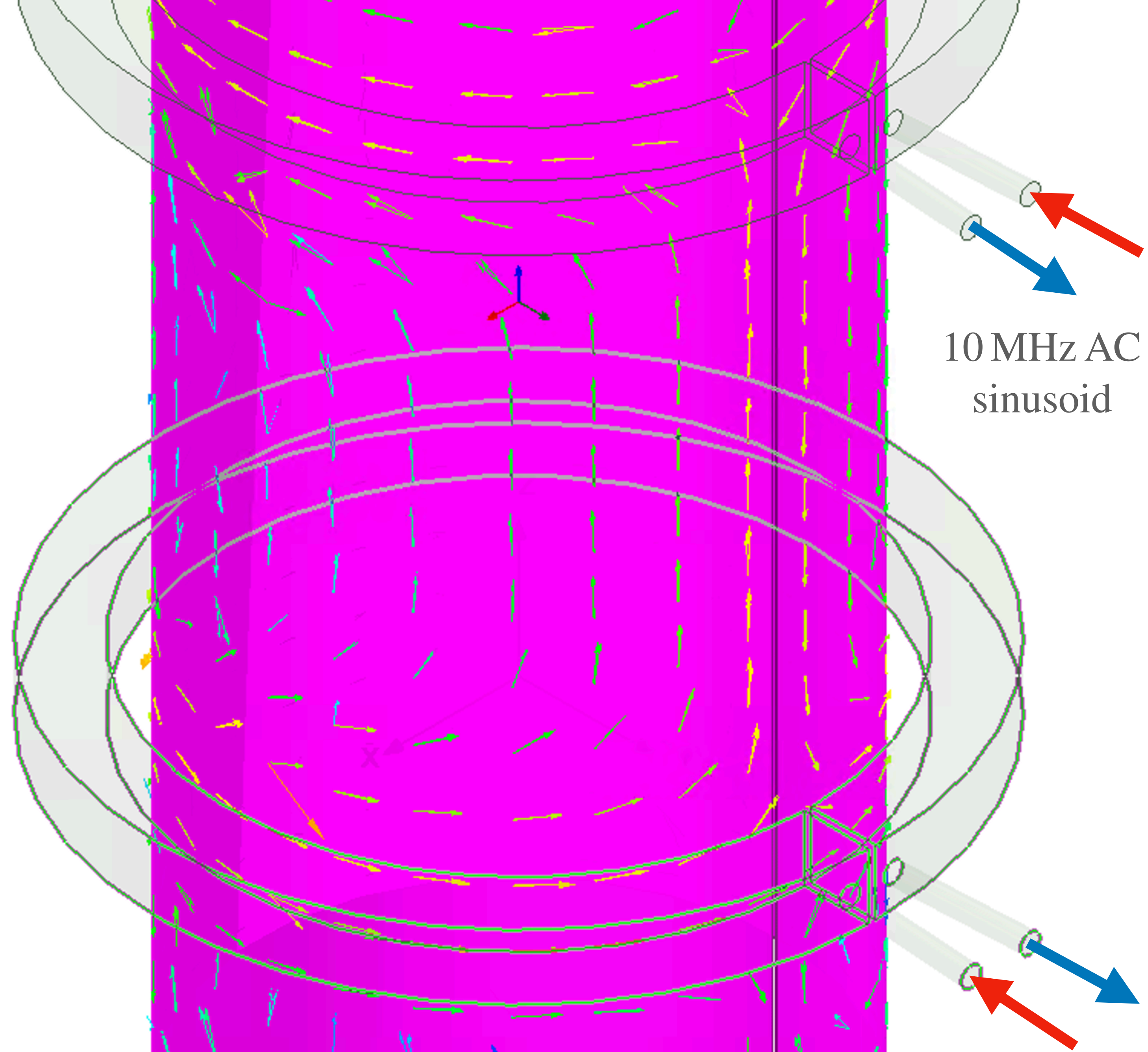
Eddy Currents & Magnetic Field Damping

- ~ 10 MHz primary frequency component
- Skin depth in aluminium:
$$\delta = \sqrt{\frac{2}{\omega\sigma\mu}} \quad , \quad \delta_{Alu}(\omega = 10 \text{ MHz}) = 65 \mu\text{m}$$
- By Lenz's Law, eddy currents are induced such that they oppose the change in the original magnetic field.
- The magnetic field seen by the muon will be suppressed.



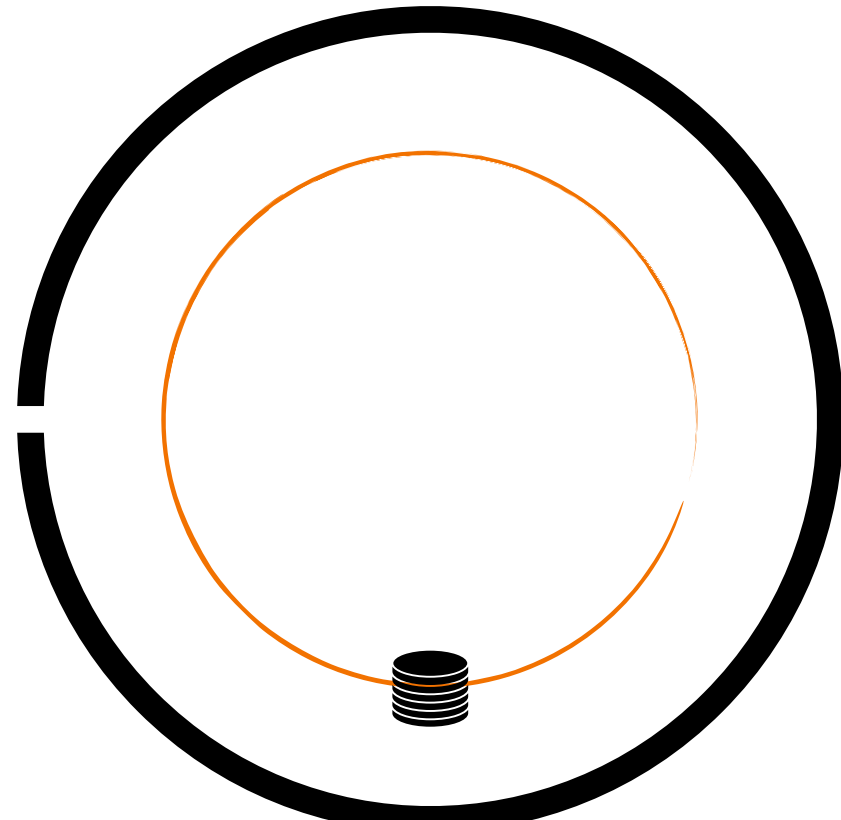
Eddy Currents & Magnetic Field Damping

- ~ 10 MHz primary frequency component
- Skin depth in aluminium:
$$\delta = \sqrt{\frac{2}{\omega\sigma\mu}} \quad , \quad \delta_{Alu}(\omega = 10 \text{ MHz}) = 65 \mu\text{m}$$
- By Lenz's Law, eddy currents are induced such that they oppose the change in the original magnetic field.
- The magnetic field seen by the muon will be suppressed.
- To achieve the field strength necessary to trap the muons in the storage region, we must:
 - Increase current
 - Optimise electrode geometry & material

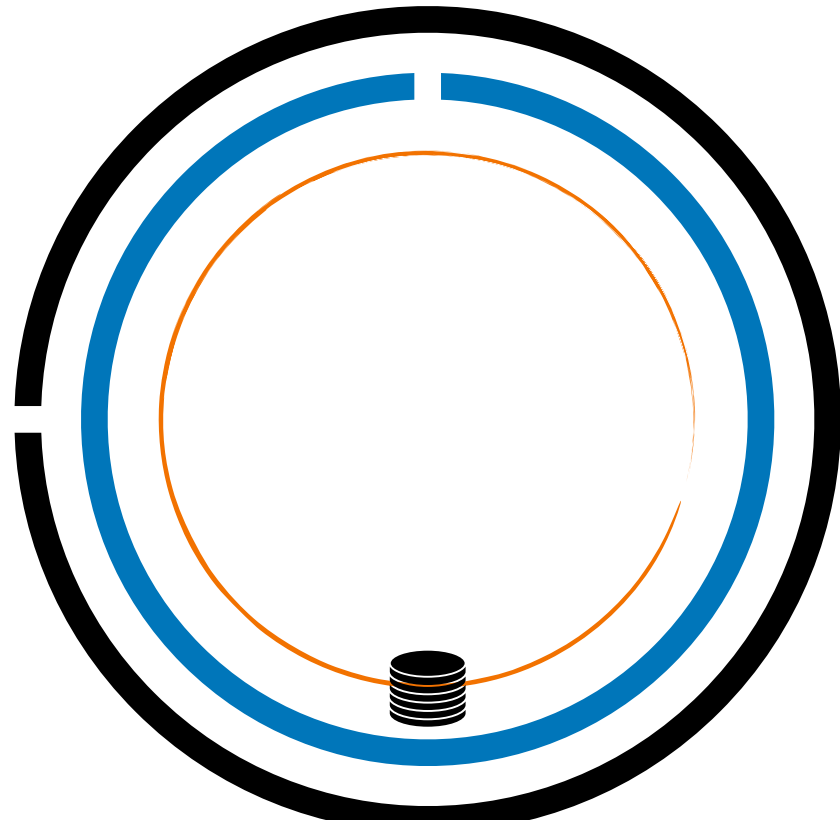


Radial Magnetic Field Measurements

- Measured using a pickup coil (🌀) at radius 30.0 ± 0.5 mm, close to the muon orbit radius.
- Different components added to observe effect, due to induction of eddy currents.



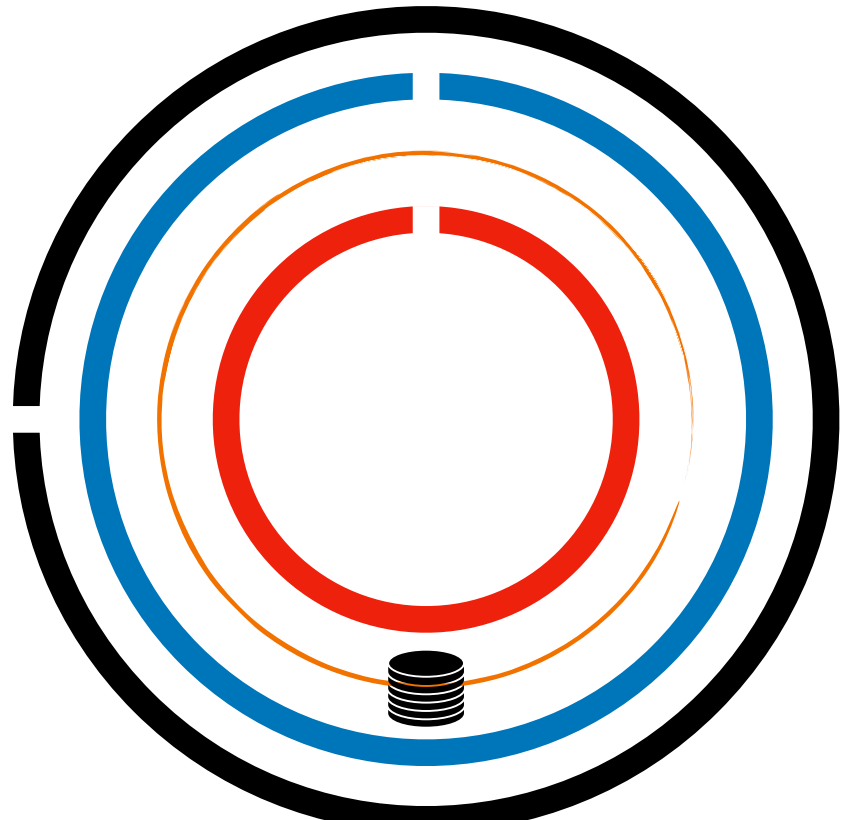
PulseCoil : Alu, $10 \times 10\text{mm}^2$, IR = 40 mm



PulseCoil : Alu, $10 \times 10\text{mm}^2$, IR = 40 mm

GND : Alu/Kapton 30 nm

$$D = 0.54 \pm 0.04$$

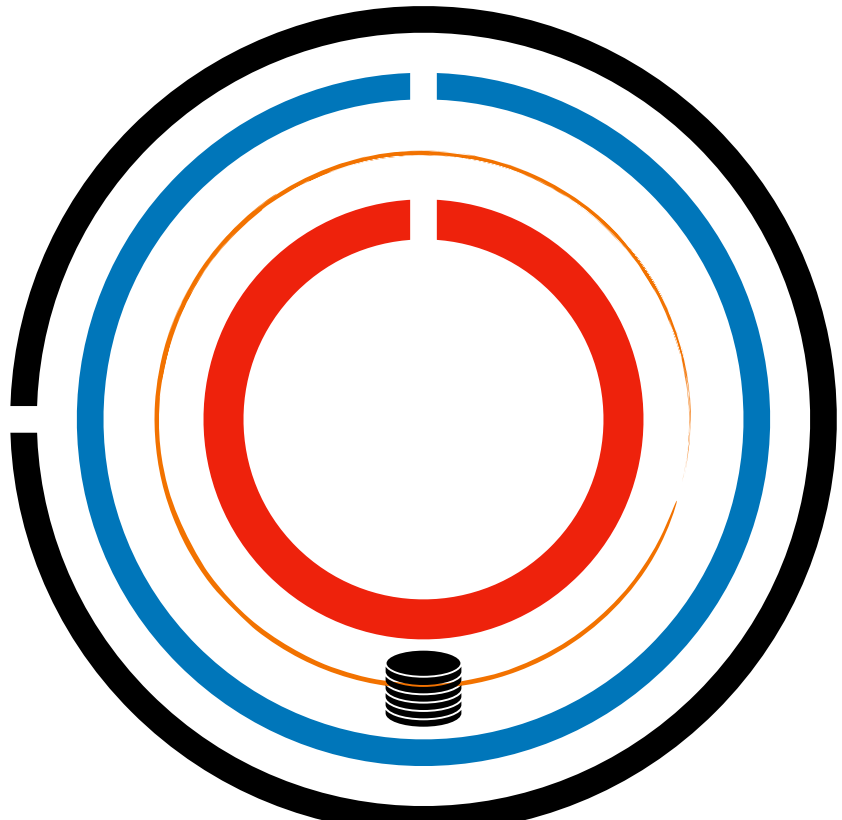


PulseCoil : Alu, $10 \times 10\text{mm}^2$, IR = 40 mm

GND : Alu/Kapton 30 nm

+HV : Alu/Kapton 30 nm

$$D(\phi_{\text{HV}} = \pi) = 0.33 \pm 0.02$$



PulseCoil : Alu, $10 \times 10\text{mm}^2$, IR = 40 mm

GND : Alu/Kapton 30 nm

+HV : Alu/Kapton 100 nm

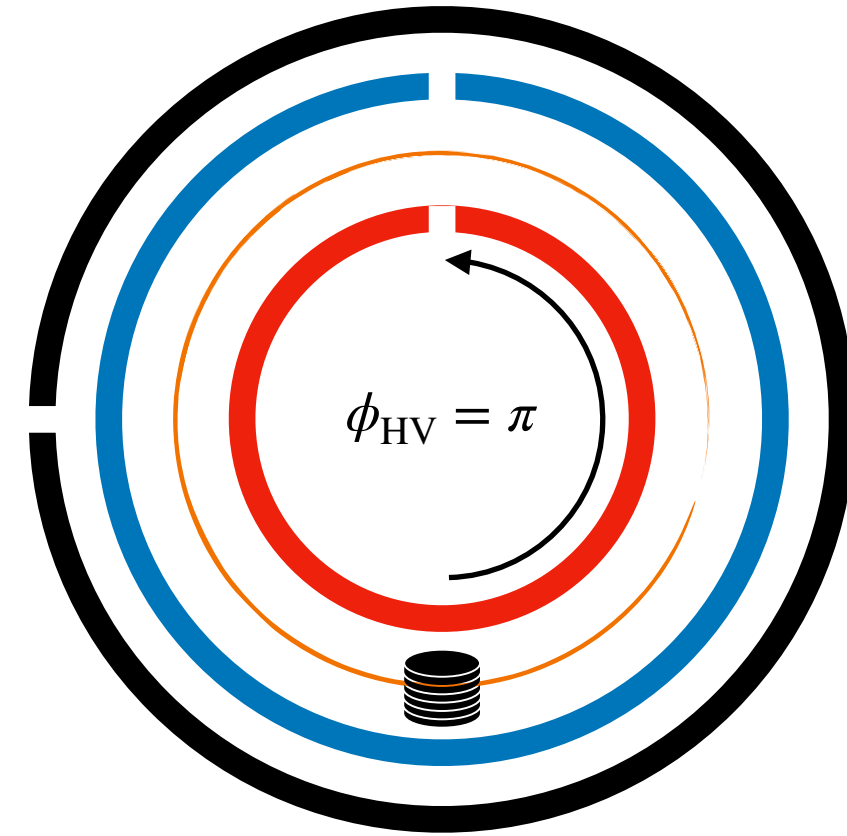
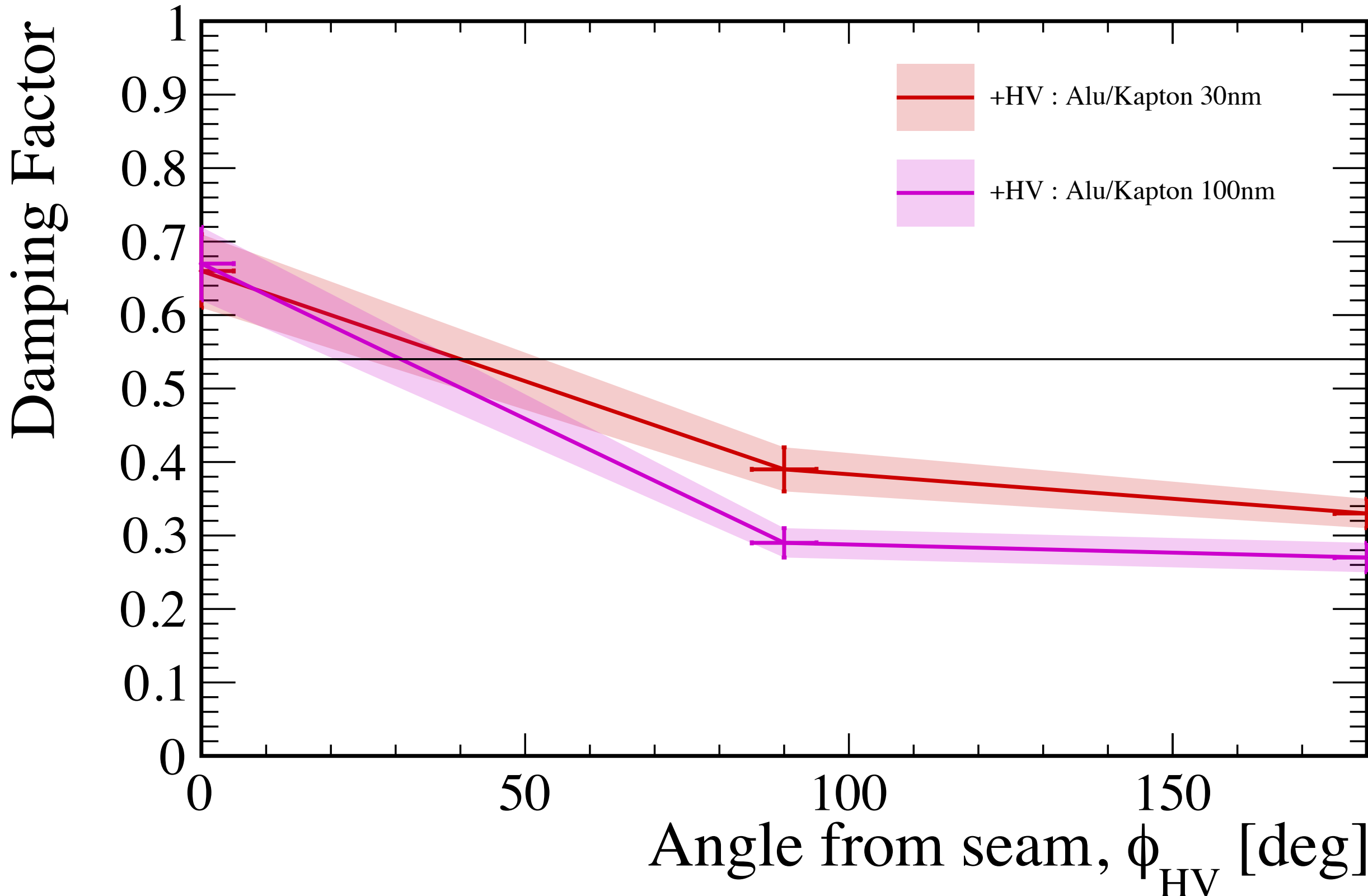
$$D(\phi_{\text{HV}} = \pi) = 0.27 \pm 0.02$$

Field Reference B_{coil}

$$\text{Damping Factor, } D = \frac{B}{B_{\text{coil}}}$$

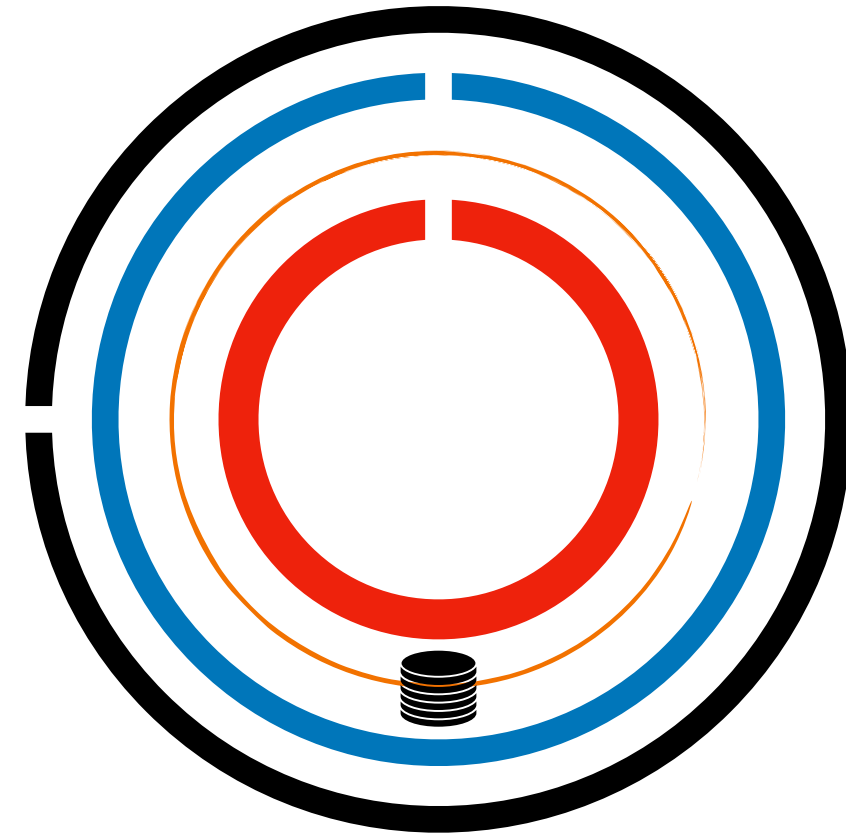
Radial Magnetic Field Measurements

- Measured using a pickup coil (🌀) at radius 30.0 ± 0.5 mm, close to the muon orbit radius.
- Different components added to observe effect, due to induction of eddy currents.



PulseCoil : Alu, $10 \times 10\text{mm}^2$, IR = 40 mm
 GND : Alu/Kapton 30 nm
 +HV : Alu/Kapton 30 nm

$D(\phi_{HV} = \pi) = 0.33 \pm 0.02$

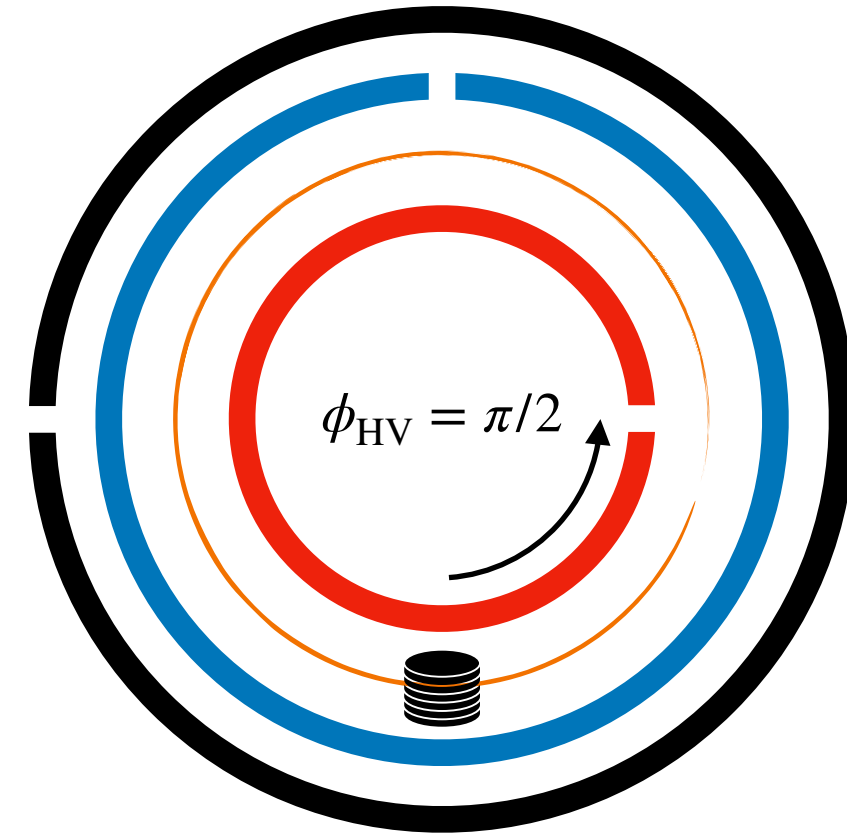
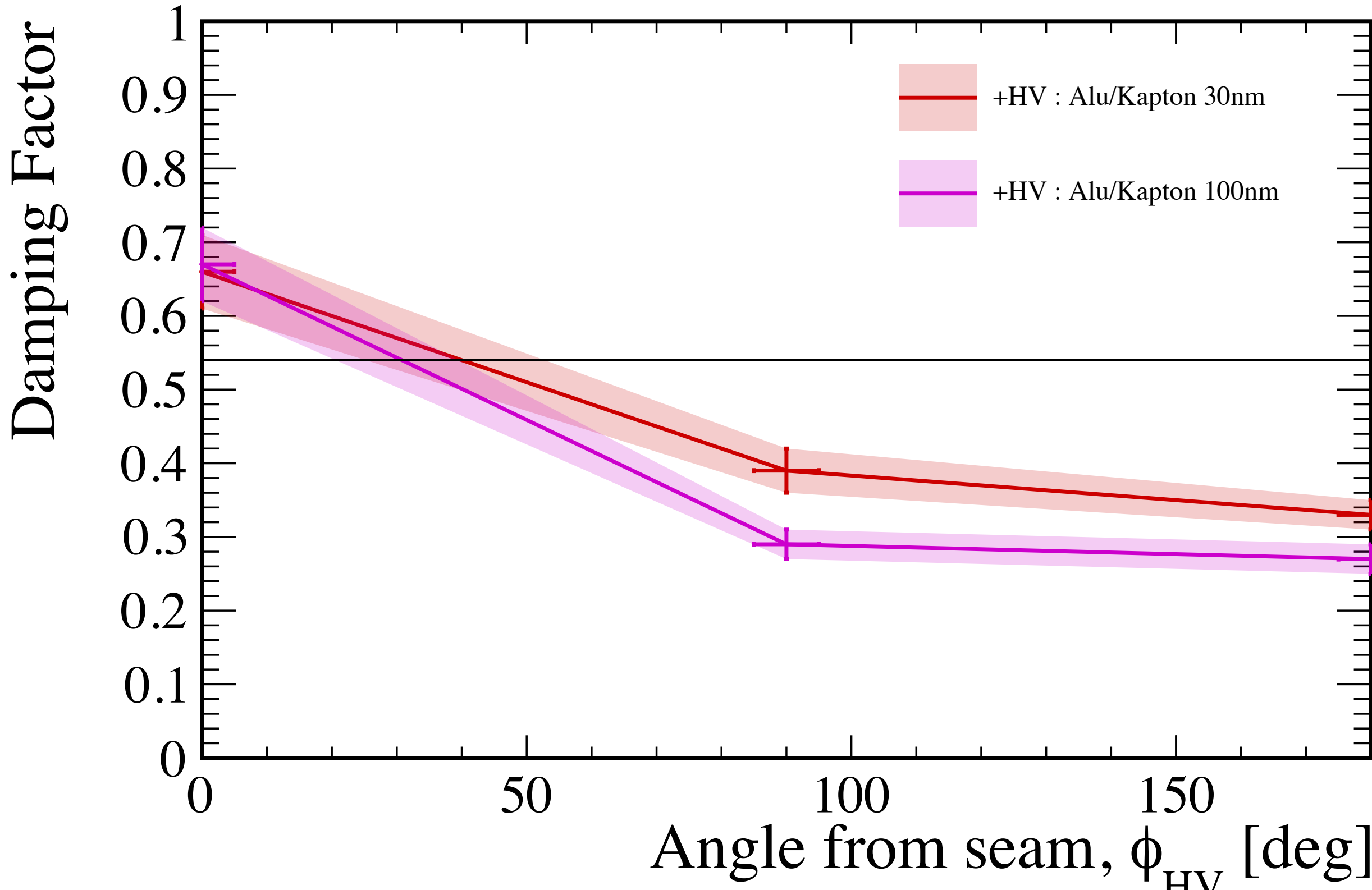


PulseCoil : Alu, $10 \times 10\text{mm}^2$, IR = 40 mm
 GND : Alu/Kapton 30 nm
 +HV : Alu/Kapton 100 nm

$D(\phi_{HV} = \pi) = 0.27 \pm 0.02$

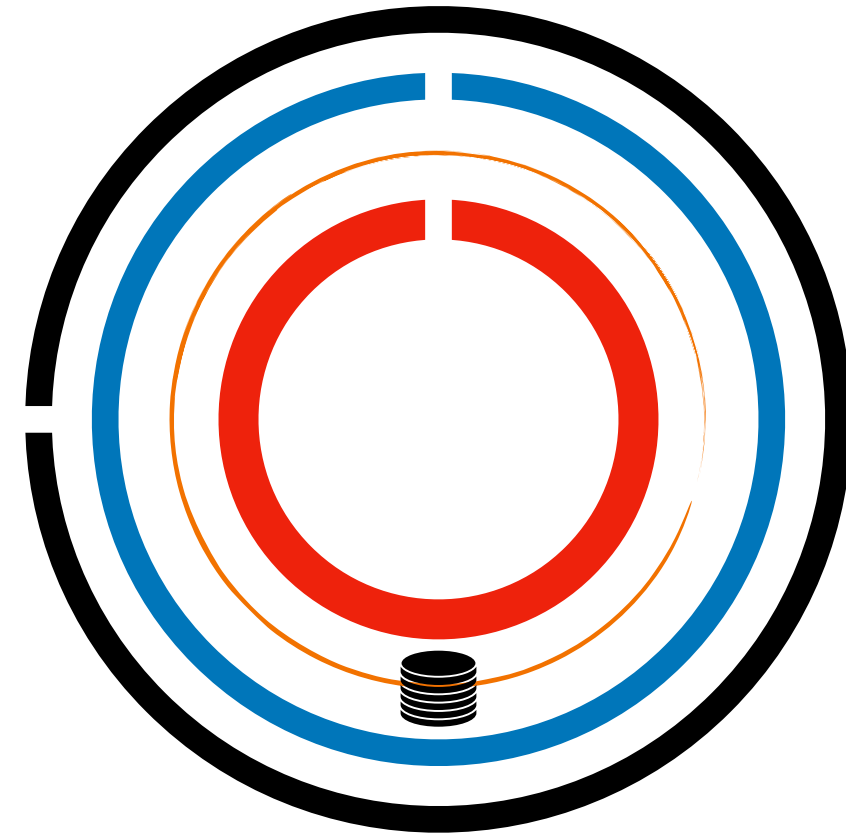
Radial Magnetic Field Measurements

- Measured using a pickup coil (🌀) at radius 30.0 ± 0.5 mm, close to the muon orbit radius.
- Different components added to observe effect, due to induction of eddy currents.



PulseCoil : Alu, $10 \times 10\text{mm}^2$, IR = 40 mm
 GND : Alu/Kapton 30 nm
 +HV : Alu/Kapton 30 nm

$D(\phi_{HV} = \pi) = 0.33 \pm 0.02$

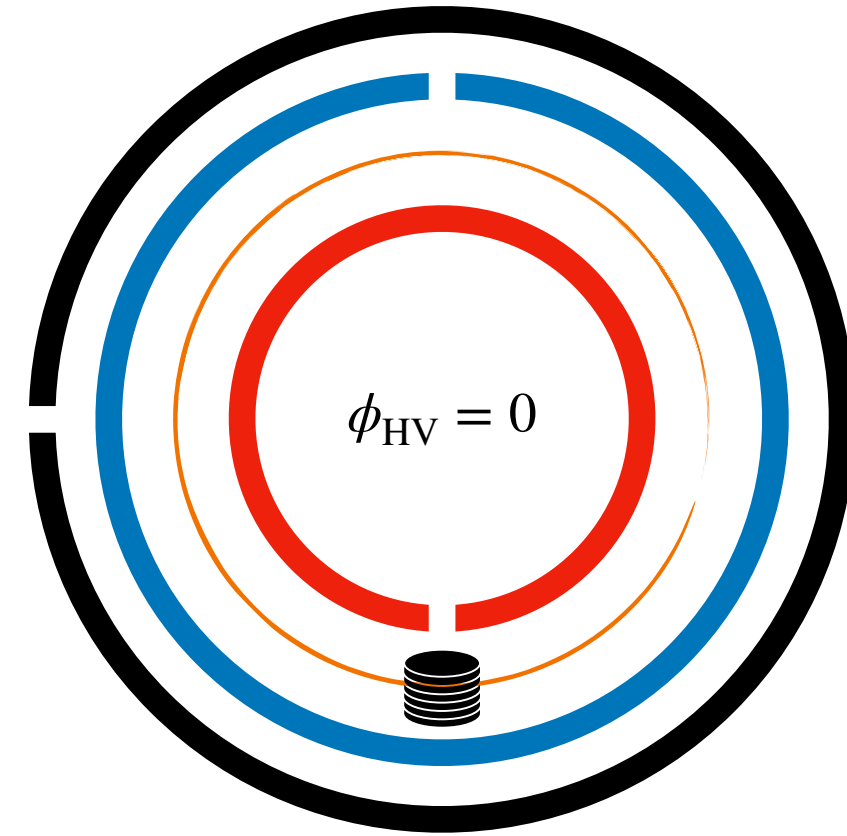
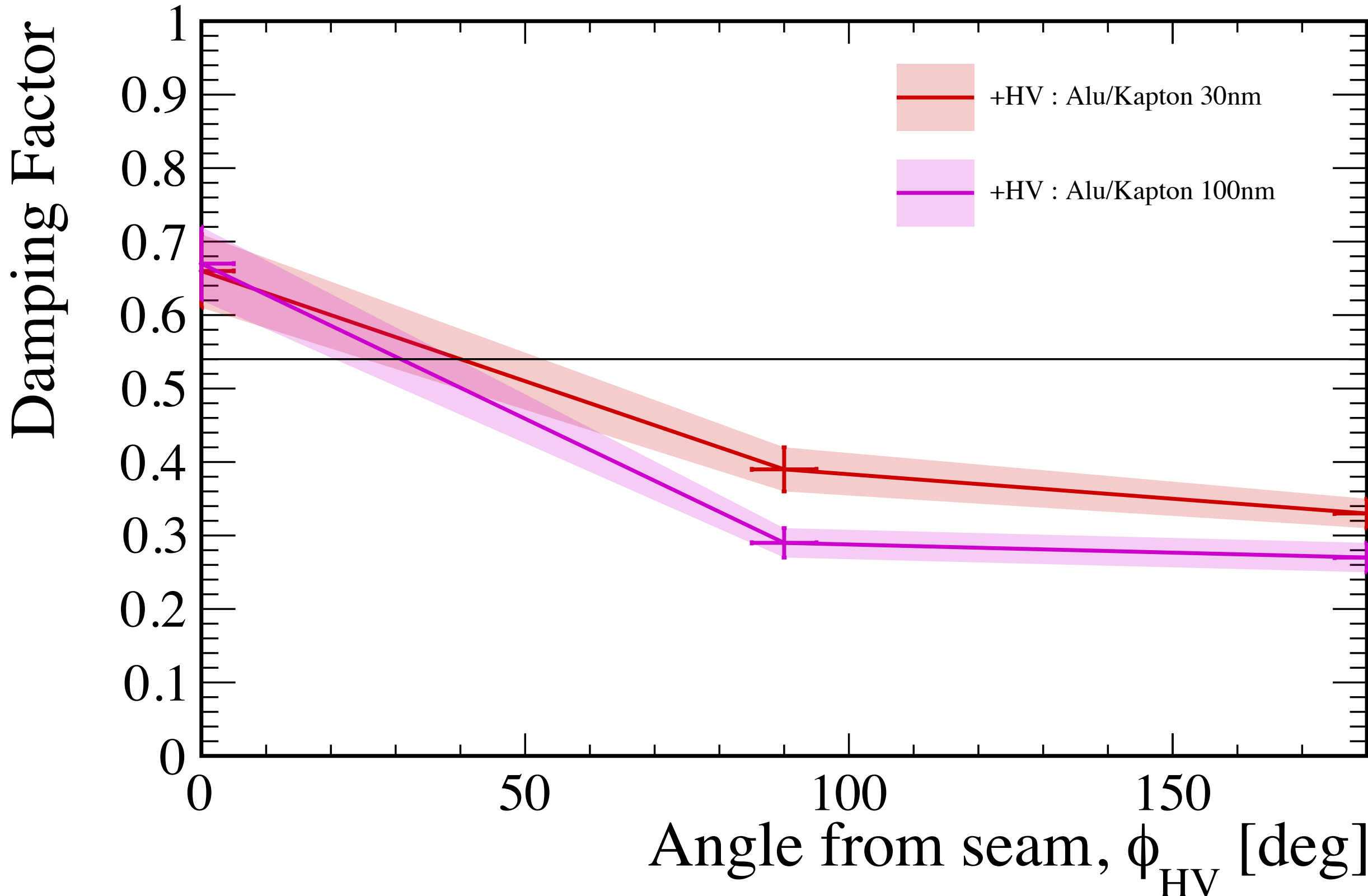


PulseCoil : Alu, $10 \times 10\text{mm}^2$, IR = 40 mm
 GND : Alu/Kapton 30 nm
 +HV : Alu/Kapton 100 nm

$D(\phi_{HV} = \pi) = 0.27 \pm 0.02$

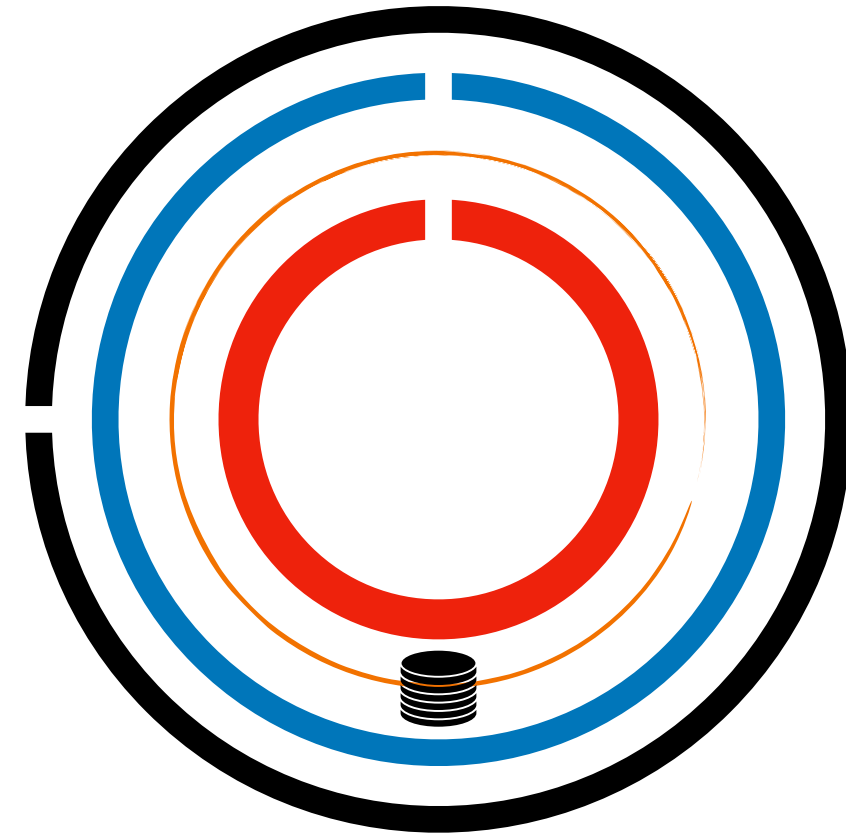
Radial Magnetic Field Measurements

- Measured using a pickup coil (🌀) at radius 30.0 ± 0.5 mm, close to the muon orbit radius.
- Different components added to observe effect, due to induction of eddy currents.



PulseCoil : Alu, $10 \times 10\text{mm}^2$, IR = 40 mm
 GND : Alu/Kapton 30 nm
 +HV : Alu/Kapton 30 nm

$D(\phi_{HV} = \pi) = 0.33 \pm 0.02$



PulseCoil : Alu, $10 \times 10\text{mm}^2$, IR = 40 mm
 GND : Alu/Kapton 30 nm
 +HV : Alu/Kapton 100 nm

$D(\phi_{HV} = \pi) = 0.27 \pm 0.02$

Summary

- The frozen-spin technique cancels the spin precession due to the anomalous magnetic moment ($g-2$), using a radial E field, leaving the EDM as the only inherent source of precession.
- The muon must be trapped in a compact stable orbit at the centre of a solenoid and the E fields precisely aligned.
- First prototypes of pulse coils and electrodes have been constructed for exploring feasible design concepts and verifying key parameters.
- Uniformity of thin foil electrode in first prototype gives encouragement that the alignment requirements (for reducing systematic effects) can be realised.
- Magnetic field damping has been estimated, informing a safety factor for the peak current of the pulse generator.
- Alternative geometries and foil types are now under investigation.

Thanks to all contributors to the muEDM Experiment

...with thanks in particular to everyone involved in prototype development related to the frozen-spin implementation:

F. Barchetti¹, R. Senn¹

R. Chakraborty¹, A. Doinaki^{1,2},
C. Dutsov¹, K. Michielsenki^{1,2}

K. Kirch^{1,2}, P. Schmidt-Wellenburg¹

1) Paul Scherrer Institute; 2) ETH Zürich;

Project funded by



Schweizerische Eidgenossenschaft
Confédération suisse
Confederazione Svizzera
Confederaziun svizra

Swiss Confederation

Federal Department of Economic Affairs,
Education and Research EAER
**State Secretariat for Education,
Research and Innovation SERI**